

# Binary black holes and tori in AGN

## II. Can stellar winds constitute a dusty torus?

C. Zier and P. L. Biermann

Max-Planck Institut für Radioastronomie (MPIfR), Bonn, Auf dem Hügel 69, D-53121 Bonn  
email: chzier@mpifr-bonn.mpg.de

May 21, 2019

**Abstract.** In this second paper, in a series of two, we determine the properties of the stellar torus that we showed in the first paper to result as a product of two merging black holes. If the surrounding stellar cluster is as massive as the binary black hole, the torque acting on the stars ejects a fraction which extracts the binary's angular momentum. After the black holes coalesced on scales of  $\sim 10^7$  yr, a geometrically thick torus remained. In the present article we show that a certain fraction of the stars has winds, shaped into elongated tails by the central radiation pressure, which are optically thick for line of sights aligned with them. These stars are sufficiently numerous to achieve a covering factor of 1, so that the complete torus is optically thick. This patchy structured torus is then compared with observations. We find the parameters of such a torus to be just in the right range in order to explain the observed large column densities in AGN and their temporal variations on time scales of about a decade. Within this model the broad absorption line quasars can be interpreted as quasars seen at intermediate inclination angles, with the line of sight grazing the edge of the torus. The half-opening angle of the torus is wider for major mergers and thus correlates with the central luminosity, as has been suggested previously. In this picture the spin of the merged black hole is possibly dominated by the orbital angular momentum of the binary. Thus the spin of the merged black hole points into a new direction, and consequently the jet experiences a spin-flip according to the spin-paradigm. This re-orientation could be an explanation for the X-shaped radio galaxies, and the advancing of a new jet through the ambient medium for Compact Symmetric Objects.

**Key words.** Dust Torus – AGN – Black Holes – Mergers – Galaxies

### 1. Introduction

Active galactic nuclei (AGN) produce very high luminosities in a very restricted volume, probably via an accretion disk around a massive black hole (BH) in which shear stresses cause matter to sink down in the potential of the BH. These luminous nuclei appear in many different flavours what the unification scheme traces back to a non-spherical symmetry of the nucleus, which is spatially not resolved. Thus the same object looks different if viewed from different directions, leading to various classifications. Now observations from radio to hard X-rays and their variability in time put certain constraints on the properties of the nuclei, which in fact are thought to be cylindrically symmetric. The rapid variation of X-rays on scales of  $10^4$  s restricts their origin to a volume of about  $3 \times 10^{12}$  m radial extension, which corresponds to the last stable orbit of a black hole of  $\sim 3 \times 10^8 M_{\odot}$ . The ultra violet (UV) and optical part of the spectrum is thought to be thermal ( $10^4$ – $10^5$  K) and generated further outside in the accretion

disk. The AGN also show broad emission lines (BL), which are observed in objects classified as Type 1, and have line widths corresponding to doppler-broadening with velocities of 1500 up to 30 000 km/s. Also these lines are varying on scales of weeks or months. Both these findings locate their origin, the broad emission line region (BLR), in a distance to the BH of up to 0.01 pc. The narrow emission lines (NL), which are detected in both classifications (i.e. Type 1 and 2), have line widths implying velocities of the order of 1000 km/s and show no variability. Thus the narrow emission line region (NLR) has a large extension, up to the kilo parsec scale.

In the infrared (IR) the spectrum shows a bump between  $2 \mu\text{m}$  and 1 mm which is thought to be due to re-radiation by dust. If the IR emission were emitted from a region comparable in size to that of its energy source, the brightness temperature would be too high to allow for thermal emission. If this emission is thermal, the black body limits the size of the source at  $1 \mu\text{m}$  and  $60 \mu\text{m}$  to 0.5 pc and more than 1 kpc respectively for the most lumi-

nous sources, while the limits for the least luminous ones are 0.01 pc and 20 pc (Sanders et al. 1989).

Now in objects classified as Type 1, all these parts of the spectrum are observed, so that the line of sight (LOS) can directly reach the central parts without matter in between blocking the view. That is different for the sources of Type 2, where there is no convincing evidence for the optical-UV emission as in Type 1s. Also the soft X-rays seem to be heavily absorbed and there are no broad emission lines detected. The unification scheme relates these differences to different orientations of the cylindrically symmetric nuclei and not to intrinsic differences.

The sketch Fig. 1 tries to illustrate the situation in double logarithmic scales, which actually maps a circle to a square. But for reasons of clarity we ignored this. In the very center is a massive BH of about  $10^8 M_{\odot}$  with a Schwarzschild radius of about  $10^{-5}$  pc. It is surrounded by an accretion disk extending to about  $10^{-3}$  pc, which produces the optical-UV emission and maybe also the X-rays. Further outside, up to 0.01 pc, the BLR is found (Peterson 1993), which is thought to be made up by clouds moving at high velocities around the central BH. This structure is surrounded by a molecular dusty torus with an inner radius on scales of about one parsec and whose axis is aligned with that of the accretion disk. At distances up to kilo parsecs the NLR is found. The so called radio loud quasars and galaxies show a strong jet emanating along the symmetry axis outwards at relativistic speeds. The dichotomy of radio loud (RL) and radio quiet (RQ) objects is suspected to be due to the spin of the central massive BH, with AGN having fast spinning black holes in their centers being able to develop powerful radio jets. Apart from their radio emission both classes show basically the same spectral features discussed above.

If our angle to the symmetry axis of an observed nucleus is in the plane of the torus, only the NLR is visible unabsorbed and in fact indistinguishable from that of Type 1 objects. The other parts of the spectrum are hidden by the torus and we classify the source as Type 2. This idea is very strongly supported by spectrapolarimetry, which reveals in the polarized spectrum of Type 2 sources a clear spectrum of Type 1 (Antonucci & Miller 1985; Miller, Goodrich, & Mathews 1991), with the power-law continuum having the same degree of polarization as the permitted broad lines, which also have normal equivalent width. The degree of polarization is found to be almost wavelength independent. This is interpreted as the reflection of the obscured Type 1 continuum by free electrons in the opening of the torus (Antonucci (1993) and references therein). And indeed, ionized matter has been observed in the opening cone of the torus, which reflects the light from the center into the line of sight of the observer, producing the right polarization. This electron scattering region (ESR) is located somewhere between the BLR and extends to scales of the height of the torus (Taniguchi & Anabuki 1999). Thus, as the viewing angle decreases, the core spectrum becomes less obscured and the LOS finally grazes the edge of the torus, with a reddened spectrum

becoming visible. The broad lines appear in the observed spectrum and the nucleus is classified as reddened Type 1 or to be of intermediate Type (gradually decreasing from Type 2 to 1 as the inclination decreases). When the inclination angle has become small enough, so that the source is almost seen face or pole on, all features of a Type 1 spectrum are visible.

In radio loud galaxies the steep synchrotron emission of the extended radio lobes of the jet becomes less prominent as the inclination angle decreases, and the flat-spectrum compact emission of the core becomes visible. The Blazars and BL Lacs are dominated by a single non-thermal spectrum with weak or no emission lines. They are explained as being dominated by emission from a relativistic jet seen face on.

In radio quiet objects there exist high luminosity AGN, the radio quiet quasars, and nuclei of much lower luminosity but showing the the same features, the Seyfert galaxies. While for the Seyferts the unification of Type 1 and 2 due to orientation effects has been established for quite some time, there was or even is still some disagreement about the existence or non-existence of Type 2 quasars. But there now seems to be strong evidence, that at least some of the ultra luminous infrared galaxies (ULIRGs) are in fact quasars of Type 2, harbouring luminous Type 1 cores in their center. For more detailed information on this issue, see Antonucci (2001b).

In case of the radio louds the powerful objects are referred to as Blazars if seen face on, radio loud quasars at intermediate angles with clearly visible Type 1 spectrum, and as Fanaroff-Riley (FR) II radio galaxies if seen edge on. Of the latter class the powerful narrow line radio galaxies (NLRG) are thought to be the Type 2 radio loud quasars. The lower luminosity radio loud objects are BL Lacs (pole on), and FR I radio galaxies (edge on).

For a much more detailed explanation of the unified scheme see for example the reviews by Antonucci (1993), Urry & Padovani (1995) and Wills (1999).

According to this scheme one essential component is the obscuring torus. Other models for such a torus either use magnetic pressure (Lovellace, Romanova, & Biermann 1998) to support the vertical thickness or radiation pressure (Pier & Krolik 1992b). Here we want to further develop our idea, introduced in a previous paper (Zier & Biermann 2001), that this torus is comprised of the winds of stars moving in the potential of a merging binary black hole (BBH), allowing them to maintain the geometrical thickness of the torus.

In that article we simulated the evolution of a stellar cluster under the influence of a massive binary black hole in its center, based on the two widely accepted assumptions that (a) galaxies with an active nucleus harbour a supermassive black hole in their center and (b) that galaxies frequently merge. The results clearly showed that the binary merges on scales of some  $10^7$  yr due to ejection of a fraction of stars, if the surrounding stellar cluster is about as massive as the binary, and ensuing emission of gravitational radiation. The stars which remained bound indeed

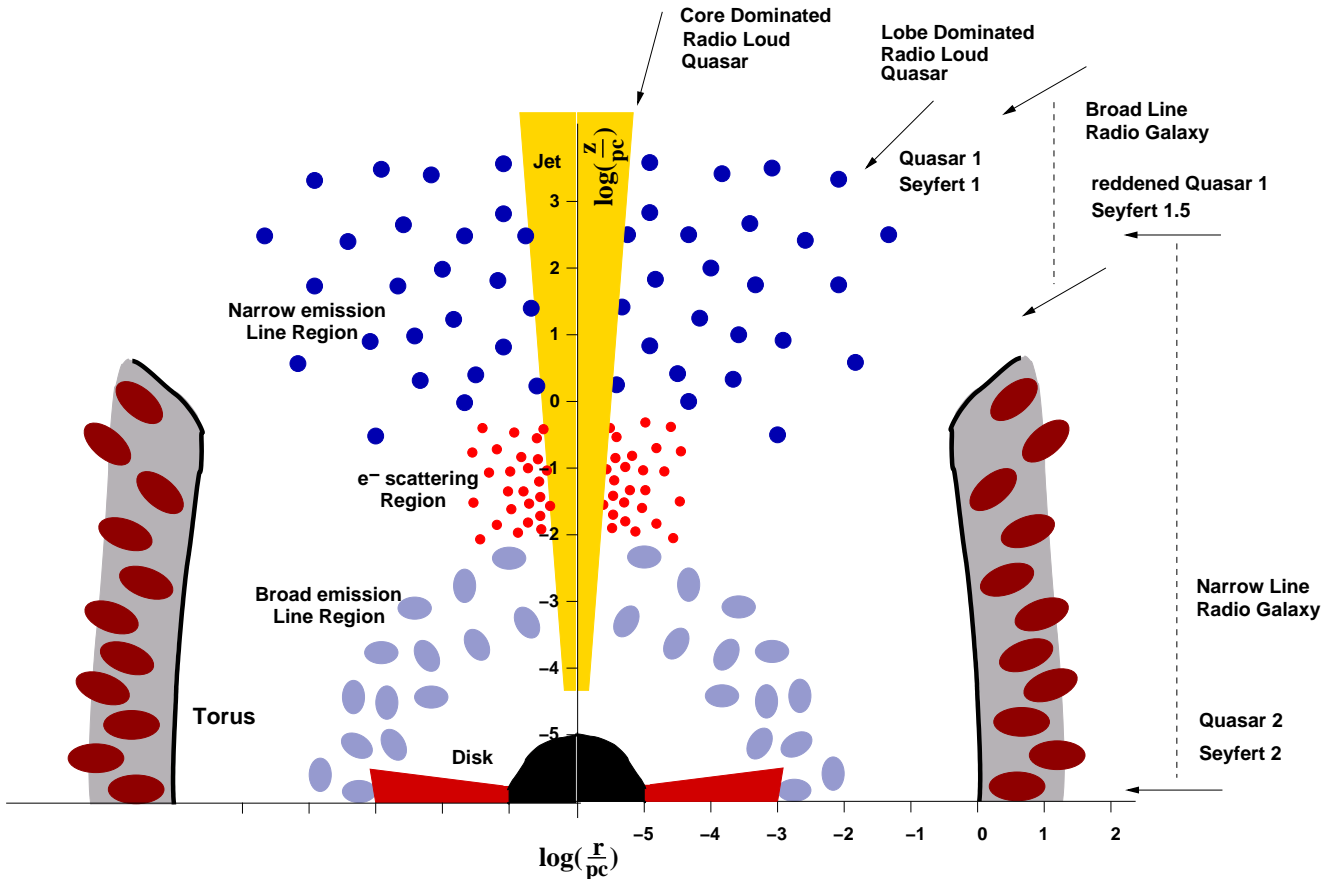


**Fig. 1.** A sketch of the cylindrically symmetric AGN according to the description in the introduction and to the picture of a patchy torus in AGN, developed in paper I and this work, is shown. The cut shows the  $r - z$ -plane, both axes logarithmically scaled to 1 pc. The basic constituents are the central BH with a surrounding accretion disk, the jet perpendicular to the disk and the torus encircling this configuration. The dark patches in the torus indicate the clouds, made up by stellar winds in our proposed concept. The locations of the BLR, ESR and NLR are shown on the left, as well as the appearance of the nucleus as a function of the angle of the LOS to the jet-axis (on the right). See text for details. Note that a strictly spherical distribution is almost a square box in this diagram.

are found to be distributed geometrically in the volume of a thick torus. In this second paper we will investigate, whether such a stellar torus can explain the presence of the ubiquitous torus surrounding apparently all AGN.

The next section will briefly review the constraints put on the properties of the torus by observations.

## 2. Properties of the torus

Although the current telescopes are not able to spatially resolve the torus in AGN, conclusions could be drawn from observations in various wave bands about the torus' geometry as well as the matter it is made of.

### *The inner radius*

The central regions of many AGN appear to contain obscuring material, probably in form of dust, that prevents IR to UV light from penetrating along covered lines of sight, see e.g. Rowan-Robinson (1977). As said in the introduction, the IR observations are consistent with dust in

some parsec distance to the center, heated to its evaporation temperature ( $\sim 1500$  K) due to absorption of the central radiation (Chini, Kreysa, & Biermann 1989; Sanders et al. 1989). Reprocessing of the primary optical-UV radiation by dust, first suggested by Rees et al. (1969), is the only plausible explanation for the steep rise of the spectrum between 1000 and  $100 \mu\text{m}$  (Engargiola et al. 1988; Chini, Kreysa, & Biermann 1989; Lawrence 1991; Hughes et al. 1993), and can not be explained by non-thermal models. But it is a hard task to estimate the contribution of thermal dust, i.e. the IR emission of non-stellar origin, for starburst regions are thought to surround the torus or are located even within the torus. See on this topic for example the more recent papers by Alonso-Herrero et al. (2001) and Laurent et al. (2000) or the review by Sanders & Mirabel (1996).

Inside the evaporation radius dust can not exist and Lawrence (1991) assumed this to be the inner radius of the dusty torus. This radius is about 1 pc, corresponding to the distance where the BBH becomes hard (Milosavljević & Merritt 2001) and what also marks the inner radius of

the torus that we obtained in our simulations (paper I). This value is also in agreement with the inner radius obtained by Krolik & Begelman (1988) from the balance between cloud evaporation by central radiation and inflow by dissipative processes in the torus. In several Type 1 AGN variations in the near-infrared (NIR) emission have been observed to lag those at shorter wavelengths (Clavel, Wamsteker, & Glass 1989; Sitko 1991; Baribaud et al. 1992). These time delays place the IR emission source in a distance from the central engine which is consistent with that of optically thin nuclear heated dust at its evaporation temperature.

To explain the bump in the near-infrared in terms of thermal dust emission, a range in the grain temperature is required ( $1500 \text{ K} \lesssim T_{\text{dust}} \lesssim 30 \text{ K}$ ), since isothermal dust close to its evaporation temperature yields a narrower bump than that observed (Sanders et al. 1989; Haas et al. 2000). Thus the torus' temperature has to decrease from the inner edge to its outer regions (Niemeyer & Biermann 1993), but a very thick and compact torus (Pier & Krolik 1992a; Pier & Krolik 1993) is not able to provide such a broad temperature range. A clumpy torus, as suggested by Krolik & Begelman (1988), has the advantage that dust in clouds can survive more easily the strong radiation field. Also, as mentioned by Efstathiou & Rowan-Robinson (1995), such a structure of the torus tends to increase the dust temperature in the outer parts since here the clouds are exposed to central radiation through gaps in the inner parts of the patchy torus. This seems also most promising to (Haas et al. 2000) in order to explain the spectral energy distribution (SED).

### Column density $N_{\text{H}}$

While the emission in the IR and from the NLR is similar in strength in Seyfert 1 and 2s and therefore assumed to be more or less isotropic, the hard X-rays are underluminous. This strongly suggests that there is absorbing matter in the line of sight to the nucleus. A lot of evidence has been accumulated on the basis of X-ray observation that the column density is in the range  $10^{22-24} \text{ cm}^{-2}$  (Mulchaey, Mushotzky, & Weaver (1992) for UV-detected Seyfert 2s), or  $1 - 8 \times 10^{24} \text{ cm}^{-2}$  (Krolik & Begelman 1988). These columns suggest lots of Seyfert galaxies to have a Thompson depth  $\gtrsim 1$ , and some absorbers even block the  $\gtrsim 10 \text{ keV}$  photons thus being Compton thick, like NGC 1068. At solar abundances this means that the column density is  $\gtrsim 10^{25} \text{ cm}^{-2}$ .

From *OSSE* observations of the Seyfert 2 galaxy NGC 4945 a column density of  $\sim 4 \times 10^{24} \text{ cm}^{-2}$  is derived (Done, Madejski, & Smith 1996; Madejski 1998). A more recent study of the X-ray observations of a sample of Seyfert 2 galaxies in the  $0.1 - 100 \text{ keV}$  spectral range with *BeppoSAX* has been performed by Maiolino et al. (1998). The sources they studied were selected according to their [OIII] optical emission line flux after correction for the extinction deduced from the Balmer decrements.

This is thought to be fairly isotropic and thus avoids a sample biased against heavily obscured nuclei, as is probably the case in former samples. Maiolino et al. (1998) find all the sources in their sample to be absorbed by column densities larger than  $4 \times 10^{23} \text{ cm}^{-2}$  and most even appear to be thick to Compton scattering with  $N_{\text{H}} \gtrsim 10^{25} \text{ cm}^{-2}$ . These sources are best described by a Compton thick cold reflection model. Hence their results provide further and strong evidence for the unification scheme and indicates that the obscuration in Type 2 AGN is probably much higher than deduced from earlier X-ray surveys. Even for three galaxies out of four observed in the Hickson-16 compact group, which have been found to harbour AGN at the low end of the luminosity scale, consistent with their small size, Turner et al. (2001) deduce from *XMM-Newton* data a heavy obscuration with columns of  $\sim 5 \times 10^{23} \text{ cm}^{-2}$ .

Reeves et al. (2001) detect a strong narrow Fe emission line at  $6.4 \text{ keV}$  with *XMM-Newton* in Mrk 205. They refer this to a substantial quantity of cool material, which is reprocessing the central radiation and reflects it into the line of sight which is not blocked since the X-ray spectrum appears to be completely unabsorbed. Assuming this cool matter to be Thomson thick and having solar Fe-abundance, the line strength requires a solid angle subtended by the cool matter of at least  $1\pi$  steradian. The most likely appearance of such matter would be in form of a molecular torus according to the unification scheme, with the hard X-rays being reflected off the inner heated surface of the torus into the line of sight. Thus the observation of the narrow Fe  $6.4 \text{ keV}$  line could provide the first evidence for Thomson thick torus in an unobscured quasar.

For the narrow line Seyfert 1 galaxy 1H 0707-495 Boller et al. (2002) report the first detection of a sharp spectral drop at  $\sim 7 \text{ keV}$  by a factor more than 2 in *XMM-Newton* data. This feature they relate to the neutral iron K-edge, but the missing of absorption at lower energies and the non-detection of the  $6.4 \text{ keV}$  Fe  $K\alpha$  emission line is not easy to interpret. The strong and rapid variability in the range of  $0.1 - 10 \text{ keV}$  suggests a direct and weakly obscured view to the center, as is expected in Type 1 AGN. Among other possible explanations the authors favour partial covering of the source by a patchy absorber with  $N_{\text{H}} \simeq 10^{21-22} \text{ cm}^{-2}$  in the line of sight. In this model the unobscured X-ray luminosity is an order of magnitude higher than that observed and another implication is the underlying very steep powerlaw ( $\Gamma \approx 3.5$ ). If the observed spectral features are in agreement with a patchy torus where the line of sight has a smaller inclination than the opening angle, or is grazing the torus' surface, this observation would strongly support the idea of a patchy torus comprised of clouds – as we suggest.

High column densities do not only result from the interpretation of X-ray observations, they have also been deduced from radio data. Conway & Blanco (1995) report on the absorption of the broad HI  $21 \text{ cm}$  line towards the compact radio nucleus of the FR II radio galaxy Cyg A. From various possibilities they favour that which ascribes

the obscuration to a torus in about 10 pc distance to a central BH of  $\sim 10^8 M_\odot$ . Assuming a spin temperature in the range 8000 – 16 000 K the authors obtain a column density in the range  $2 - 4 \times 10^{23} \text{ cm}^{-2}$ , which is in very good agreement with the column deduced from previous X-ray spectroscopy by Ueno et al. (1994), i.e.  $3.75 \times 10^{23} \text{ cm}^{-2}$ . In a later VLBI observation of Cyg A Krichbaum et al. (1998) find the flux-ratio of the jet and counter-jet,  $R = S_{\text{jet}}/S_{\text{cjet}}$ , to be a function of the frequency in the range 1.6 – 43 GHz. They explain this dependency with a partially opaque circumnuclear torus of several parsec extension, inclined to the line of sight, which partially covers the counter-jet. Thus also observations in the radio band support a patchy circum-nuclear torus.

### Opening angle

From statistical studies we know, that the radio-jet axis is uniformly distributed relative to the galaxy axis (Nagar & Wilson 1999). This is different for the orientation of the polarization vector of the scattered Type 1 spectrum and the jet axis which are either perpendicular or parallel aligned. This provides very strong evidence for a dusty torus which obscures the nucleus and belongs rather to the central region, also physically, than to the host galaxy. Obscuring dust-lanes, proposed by Malkan, Gorjian, & Tam (1998), might still contribute to the absorption of the nuclear emission, if they intersect with the line of sight (LOS).

A general tendency for the NLR to align with the radio structure is detected and observed sharply defined conical/biconical nebulae are suggestive of shadowing (Antonucci (1993) and references therein). The deficit of observed ionizing photons relative to what is needed to ionize the nebulae (Kinney et al. 1991) supports the idea of matter obscuring the central source, which is not obscured at the aspect angles, where the ionized nebulae are located. In some cases the conical or biconical structure can be seen (Pogge 1989; Wilson et al. 1993; Wilson & Tsvetanov 1994; Macchetto et al. 1994) with half-opening angles in the range of  $35^\circ$  to  $50^\circ$  and being aligned within a few degrees with the inner radio jets (Nagar & Wilson 1999). Thus it is evidently shown that the ionizing photons escape from the center in a cone whose axis is aligned with that of the radio emission so that the optical, UV and probably soft X-ray radiation is collimated by the torus, escaping anisotropically through the polar cap regions.

Using the statistics of the observed number ratios of Seyfert 1 and 2s (Osterbrock & Shaw 1988; Huchra & Burg 1992; Barthel 1989; Willott, Rawlings, & Blundell 1999) a half-opening angle of the torus in the range  $30^\circ - 60^\circ$  is obtained. This matches very well the angles of the ionization-cones inside the opening of the torus.

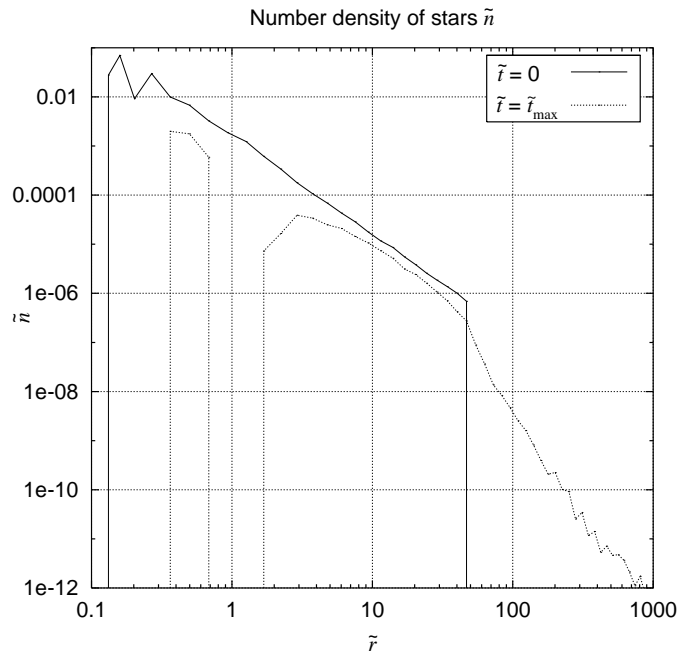


**Fig. 2.** The stellar number density distribution is shown at the beginning ( $\tilde{t} = 0$ ) and end ( $\tilde{t} = \tilde{t}_{\text{max}}$ ) of the simulation. Finally, at  $\tilde{t}_{\text{max}}$ , the bound star distribution follows a powerlaw with index  $-4$  in the heated region ( $\tilde{r} \gtrsim 50$ ), while an index  $\sim -2$  is maintained in the range  $10 \lesssim \tilde{r} \lesssim 50$ . The inner parts are scoured out due to ejection of stars by the binary, and a maximum emerges at  $\tilde{r} \approx 3$ , showing the torus-like configuration the stars assume. For  $\tilde{r} \lesssim 0.7$  a cusp of stars bound to  $M_1$  only is left.  $\tilde{r}$  is normalized to 1 pc and  $\tilde{n}$  such that the area underneath the solid line is 1.

### Covering factor

According to the opening angle of the torus, it screens a considerable fraction of the solid angle, seen from the central source, and is geometrically thick. Blocking the view to the nucleus in Type 2 AGN, the torus, if comprised of individual clouds, must be optically thick for most of the lines of sight penetrating it. Thus the clouds constituting the torus must achieve a covering factor of about one, if a single cloud is optically thick, and more otherwise.

Hence the observations demand a clumpy-structured torus with an inner radius of about 1 pc, that is optically and geometrically thick with a half-opening angle of  $\sim 45^\circ$  and therefore has a covering factor of order unity.

### 3. Kinematics and density distribution of the stars

Our simulation of a stellar distribution in the potential of the binary, that is discussed in detail in paper I (Zier & Biermann 2001), we performed for three different mass-ratios of the BHs ( $q = 1, 10, 100$ ), with

$$q = \frac{M_1}{M_2}.$$

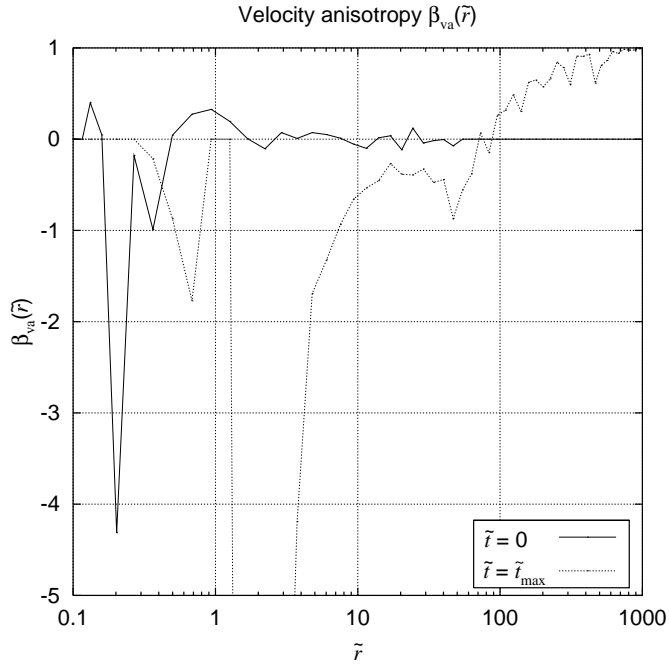


**Fig. 3.** The initial conditions ( $\tilde{t} = 0$ ) of the star cluster have been set so that the velocity anisotropy  $\beta_{\text{va}} = 1 - \frac{\langle v_\theta^2 \rangle - \langle v_r^2 \rangle}{2\langle v_r^2 \rangle}$  is neither radial ( $\geq 1$ ) nor tangential ( $\leq -1$ ) anisotropic. At  $\tilde{t} = \tilde{t}_{\text{max}}$  the velocity anisotropy of the bound stars is a strongly increasing function of the radius. In the range  $r \lesssim 50$  they are tangentially anisotropic, while in the heated region ( $r \gtrsim 50$ ) the stars are moving on radial anisotropic orbits.

where  $M_1 \geq M_2$ , always. In that article we focused on the ejected fraction of the stars and mentioned only some properties of the population of the bound stars. In this section we will discuss the bound stars and for clarity briefly summarize just a few results from paper I, using a mass-ratio of the BHs of  $q = 1$ .

### 3.1. Dynamics of the bound stars

In order to write the equations in their dimensionless form, denoted by a tilde “ $\sim$ ” on top of the quantities, we used the following normalization parameters:

$$\begin{aligned} r_0 &= a = 1 \text{ pc}, \\ t_0 &= \sqrt{\frac{r_0^3}{G(M_1 + M_2)}}, \\ L_0 &= \frac{ma^2}{t_0}. \end{aligned}$$

The semi-major axis of the BBH, used in the calculations, is denoted by  $a$ , and for the mass of a typical star  $m$  we used one solar mass.

At the end of the simulation the initial singular isothermal sphere has evolved into a distribution which is depleted in the inner regions (see Fig. 2). The stellar density peak in the center with a radial extension of about  $\tilde{r} = 0.5$

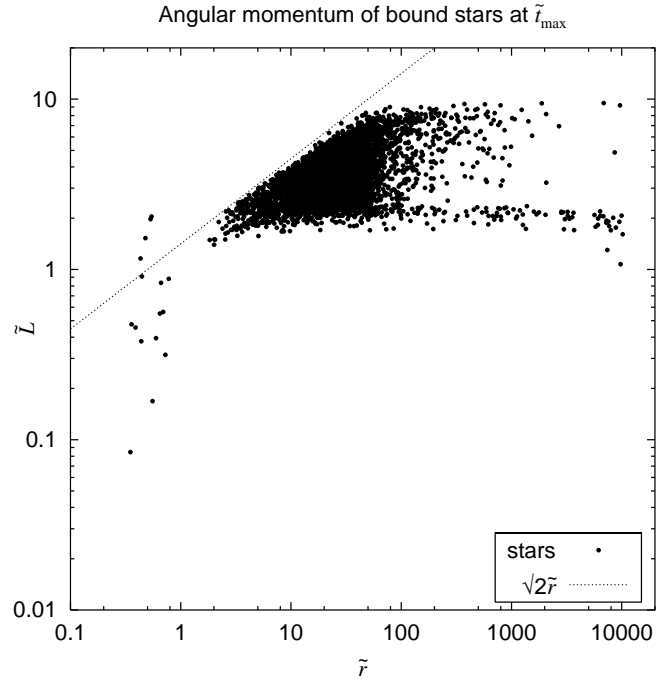


**Fig. 4.** Plotting the angular momentum  $\tilde{L}$  versus the distance  $\tilde{r}$  at  $\tilde{t}_{\text{max}}$  shows all stars to respect the upper limit indicated by the dotted line. Only some stars in the cusp region ( $\tilde{r} < 1$ ) have larger angular momenta, because they are bound to one BH only, with the other perturbing their orbits, so that the assumption of a point-mass potential does not apply at these small distances. For  $\tilde{r} \gtrsim 50$  two populations can be distinguished, one clustering around  $\tilde{L} \approx 2$  (heated stars) and the other having an upper limit of  $\tilde{L} \approx 10$ , fading towards smaller values (relaxed stars). See text for details.

is made up by a fraction less than 0.4% of the final distribution and is bound to the primary black hole only. We assume that this cusp would be much shallower if we would have allowed the BBH to shrink in the simulation, and thus will not address it further in our discussion.

After a gap in a distance corresponding to the radial distance of the secondary black hole to the center, the density increases again and peaks at  $\tilde{r} \sim 3$ . In the range  $10 \lesssim \tilde{r} \lesssim 50$  the density follows the initial powerlaw of the isothermal sphere ( $\tilde{n} \propto \tilde{r}^{-2}$ ) and for radii bigger than the outer limit of the initial distribution ( $\tilde{r} \gtrsim 50$ ) approximates a powerlaw with index  $-4$ .

In paper I we showed that the stars with small angular momenta strongly interact with the binary because of their small pericenters, which enable them to get sufficiently close to the orbit of the secondary black hole, in order to become ejected. Only stars moving on orbits with sufficiently large pericenters ( $\tilde{r}_- \gtrsim 2$ ) can remain in the central regions. The smaller their radii get, the more they are tangentially anisotropic (see Fig. 3) and the less eccentric is their orbit. But not all of the stars which initially have smaller pericenters gained enough energy as to become ejected. A fraction will be heated to larger distances

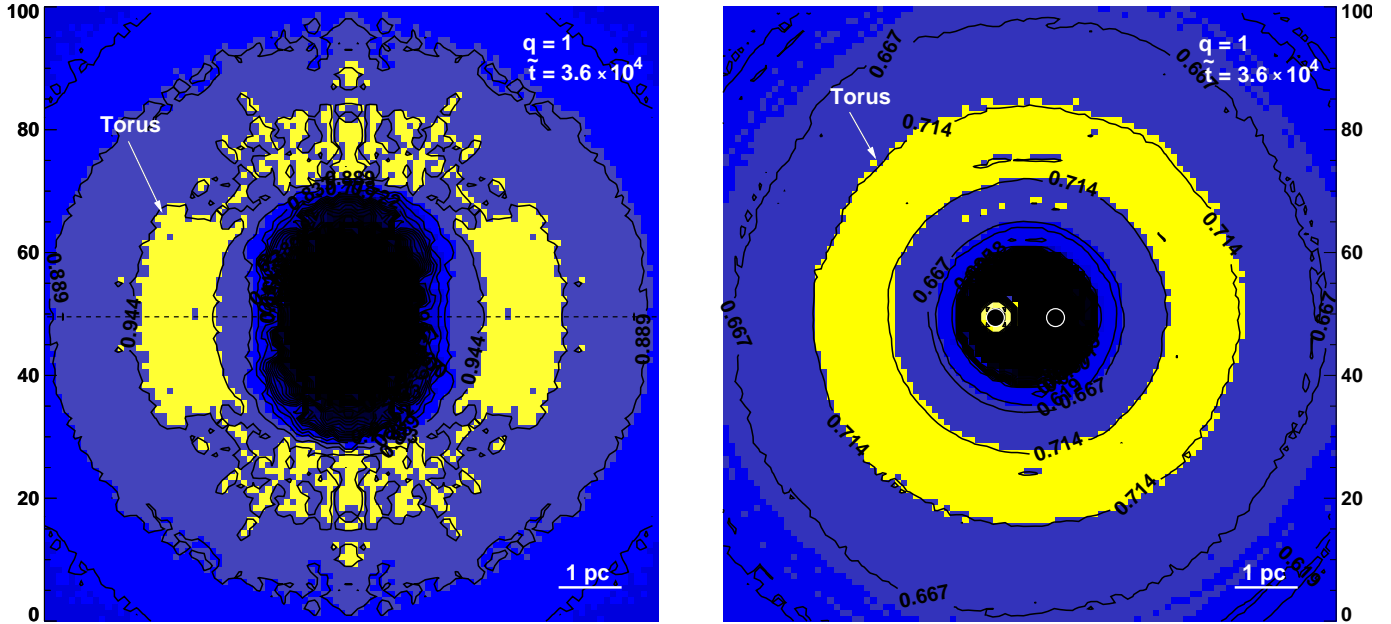


**Fig. 5.** Cuts through the stellar density in the comoving frame are shown with contours scaled logarithmically. The right panel displays the equatorial plane (BHs marked by black spots). Perpendicular to it the  $x = 0$ -plane is shown (left panel), with the  $y$ -axis drawn as dashed line, so that the BHs are in front and behind the paper-plane. The initial distribution is a gaussian and the mass-ratio is 1. After initially stars close to the orbits in 0.5 pc from the center are ejected and the polar regions are depleted, finally a torus emerges in the equatorial plane at  $r \sim 3$  pc. An expanded version of this diagram for the mass-ratio 10 is shown in paper I.

and stays bound to the binary, i.e. still has negative energies. Such stars contribute to the distribution at distances which are larger than the extension of the initial distribution, which terminates at  $\tilde{r} = 50$  (see Fig. 2).

But further outside we will not only find the heated stars originating from the central regions. Due to our initial conditions the density distribution has a sharp cutoff at  $\tilde{r} = 50$ . Among the stars close to this outer radius are also those which happen to be at, or close to their pericenters at the very beginning of the simulation. As time proceeds they are moving on their orbits without being noticeably affected by the secondary BH, whose perturbation to a point-mass potential is negligible at large distances. Thus, keeping their energy and angular momentum nearly conserved, these stars diffuse into the outer regions ( $\tilde{r} \geq 50$ ). The expansion of the initial distribution is just a process of relaxation and would have occurred also in a point-mass potential. Thus the region at  $\tilde{r} \geq 50$  is partly populated by stars which did not interact with the binary.

Both these populations can be clearly distinguished in Fig. 4, where we plotted the angular momentum versus the radius for each single star at the end of the simulation. For  $\tilde{r} \gtrsim 50$  one population is clustering around  $\tilde{L} \approx 2$  and the other having an upper limit at  $\tilde{L} \approx 10$ , fading towards smaller angular momenta. Both are extending to radii of about  $10^4$ , with the former population being more pronounced at such big distances.

In a point-mass potential the energy reads in dimensionless units

$$\tilde{E} = \frac{\tilde{v}_r^2}{2} + \frac{\tilde{L}^2}{2\tilde{r}^2} - \frac{1}{\tilde{r}}, \quad (1)$$

with the maximum value for the energy of a bound star just below zero. In order to maximize the angular momentum, all its kinetic energy is assumed to be stored in tangential motion so that  $\tilde{v}_r = 0$ . Solving now for the angular momentum results in

$$\tilde{L} < \sqrt{2\tilde{r}} \quad (2)$$

as the upper limit for bound stars. This power law with index  $-1/2$  is indicated in Fig. 4 by the dashed line.

However, the nature of the two populations at  $\tilde{r} \gtrsim 50$  can be understood easily if we calculate the maximum possible angular momentum for the stars as function of their initial pericenter. Writing this in dimensionless form gives

$$\tilde{r}_- = \frac{\tilde{L}^2}{1 + \epsilon}. \quad (3)$$

In order to obtain an upper limit for the angular momentum of the diffused population, we assume that some stars at  $\tilde{r} = 50$  are initially at their pericenter and move on highly eccentric orbits ( $\epsilon \rightarrow 1$ ). Solving equation (3) for  $\tilde{L}$  under these conditions gives the maximum angular momentum,

$$\tilde{L}_{\text{lim}} = \sqrt{2\tilde{r}_-} = 10. \quad (4)$$

If we use for the initial pericenter instead of 50 the value  $\tilde{r}_- = 2$  we obtain  $\tilde{L}_{\text{lim}} = 2$ . This clearly shows that the stars at  $\tilde{r} \gtrsim 50$ , which have angular momenta which tend to 10, initially have been close to  $\tilde{r} = 50$  and thus diffused into this region. On the other hand the stars with angular momenta  $\tilde{L} \approx 2$  had initial pericenters close to the radius of the orbit of the secondary BH and hence could undergo strong interactions with the BBH. As the ejected stars, they gained energy in such interactions which allow them to move to radii up to  $10^4$  and thus they are identified with the heated population, clustering around  $\tilde{L} \approx 2$  (Fig. 4). This shows that in fact the heated stars are very similar to the ejected stars which have been discussed in detail in paper I. Their velocity is also radially anisotropic ( $\beta_{\text{va}} > 0$ , see Fig. 3) and they are moving on highly eccentric orbits. They only did not gain sufficient energy as to escape from the binary.

This can be confirmed by computing the maximum distance a star can travel, when it is moving at escape velocity,  $\tilde{v}_{\text{esc}} = \sqrt{2/\tilde{r}}$ . If we integrate  $\tilde{v}_{\text{esc}}$  with respect to time from the beginning of the calculations till the end of the simulation ( $\tilde{t}_{\text{max}} = 5 \times 10^5$ ) this distance is

$$\tilde{r}_{\text{max}} = \left( \frac{3}{\sqrt{2}} \tilde{t}_{\text{max}} + \tilde{r}_i^{3/2} \right)^{2/3} \approx 10^4, \quad (5)$$

corresponding to the largest radii in Fig. 4. For the initial radius  $\tilde{r}_i$  we have inserted values ranging from 0 to 50, but since the first term in the brackets dominates the expression it does not make a difference whether the stars started in the center or from the edge of the initial distribution.

As we have already mentioned in paper I, the bound stars eventually assume a torus-like structure as is shown in Fig. 5, which is taken from that article. It displays cuts through the 3-dimensional density distribution in the co-moving frame of stars which initially have been distributed according to a gaussian. The right panel shows the equatorial plane ( $z = 0$ ) with the BHs marked by the black points with white frames,  $M_1$  to the right. The slice in the left panel is perpendicular to the equatorial plane and contains the  $x = 0$ -plane, with the  $y$ -axis indicated by the dashed line. The figure shows the density distribution after about  $10^7$  yr, when the BHs have merged (see paper I). The central parts have been scoured out and a torus in the equatorial plane of the binary with a radius of about 3 pc is left. The basic topology of the final density distribution can be understood in physical terms, where we consider the torque exerted by the two black holes on an orbiting star. Fig. 3 in paper I shows of the normalized torque the component  $\tilde{L}_{z,1}/\tilde{r} = \tilde{r}\ddot{\phi}\sin^2(\theta)$  relative to the  $z$ -axis of the BBH as a function of time for different angles  $\theta$  between the rotation axis of the BBH and the symmetry axis of the star's orbit. The bigger the angle  $\theta$  is (i.e. for orbits through the polar regions), the more is the star's trajectory disturbed by the influence of the two BHs. The cumulative effect of these large excursions in the polar cap regions deplete the stellar population leaving a torus behind.

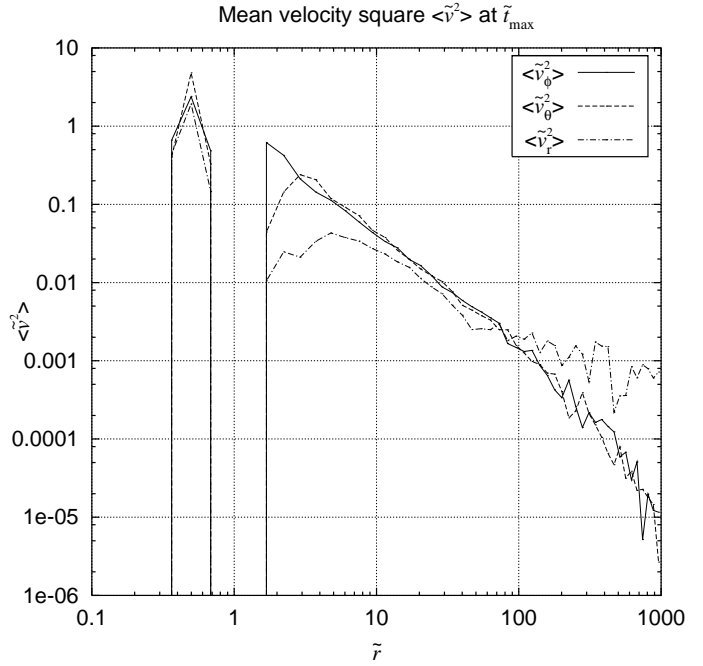


**Fig. 6.** The mean of the squares of the velocity components in spherical coordinates are displayed at  $\tilde{r}_{\text{max}}$ . In the range of the initial distribution ( $\tilde{r} \leq 50$ ) both tangential components exceed the radial one, while at larger distances it is just the opposite, in accordance with Fig. 3. In the range from the inner edge of the torus at  $\tilde{r} = 1$  to the maximum of the number density at  $\tilde{r} = 3$  (Fig. 2), the azimuthal component is larger than  $\langle \tilde{v}_\theta^2 \rangle$ , in favour of the toroidal distribution of the stars. At larger distances these components become indistinguishable.

For a single star moving on an orbit which is inclined by the angle  $\theta$  to the equatorial plane the tangential velocity components are

$$\begin{aligned} \tilde{v}_\phi &= \tilde{v}_t \cos \theta_v \\ \tilde{v}_\theta &= \tilde{v}_t \sin \theta_v, \end{aligned}$$

where  $\theta_v$  is the angle enclosed by the binary's rotation axis and the velocity-vector  $\mathbf{v}$  of the star. Thus the total tangential velocity component is  $\tilde{v}_t = (\tilde{v}_\phi^2 + \tilde{v}_\theta^2)^{1/2}$ . If we now assume the stars to be constrained to a torus-like volume as is suggested by Fig. 5, we would expect their azimuthal velocity component  $\tilde{v}_\phi$  to exceed the polar component  $\tilde{v}_\theta$ . This is verified in Fig. 6, where we have plotted the mean square of each velocity component versus the radius: At the inner edge of the torus between 1 and 2 pc distance (Figs. 2 and 5) the mean square of the azimuthal component is a factor of about 10 larger than  $\langle \tilde{v}_\theta^2 \rangle$ . With increasing radius both components approach each other and at about 8 pc they are almost indistinguishable. Hence the toroidal structure which the bound population assumes once the BHs are merged is confirmed also by the kinematics of the stellar distribution.

#### 4. Stellar winds comprising a patchy torus

Now that eventually the bound stars indeed constitute a torus-like distribution which is geometrically thick, just as required by the unification scheme, we may ask about the effects of this structure on the radiation emitted from the center inside the stellar distribution. Of course the stars alone are not able to obscure this radiation, since at a distance of about  $r = 3$  pc a number of order of at least  $(r/R_*)^2 \approx 10^{12}$  stars would be required to achieve a covering factor of order of unity. For this estimation we used giant stars with a radius of  $10^{11}$  m. But if there is a sufficiently large number of stars in the torus with dense winds which absorb a significant fraction of the central radiation, the complete torus might be opaque. To get an estimate of the optical depth and density of the torus we have to examine its constituents, the stars and their winds, more closely.

Solar type stars are not appropriate for the obscuration of the AGN, since their winds are too weak. But there are various other stars which can account for the obscuration and which we will call ‘obscuring stars’ (OS) in the following. Using evolutionary tracks, Young, Shields, & Wheeler (1977) showed that the total fraction on the giant branch in a cluster ranges between 1% and 2% for an interval 1 to 5 billion years after coeval star formation. In a first paper Shull (1983) assumed a dense stellar cluster to consist of two components, one evolved component of red giants ( $1 M_\odot$ ,  $100 R_\odot$ ) comprising 1% of the stars, and a main-sequence component. In a later paper (Voit & Shull 1988) the fraction of supergiants in a thermal cluster was assumed to comprise only 0.01%, giants ( $1 M_\odot$ ,  $10 R_\odot$ ) 1% and the rest of the cluster to be made up by main-sequence stars. This would be only a small fraction with stars having mass-loss rates of typically  $10^{-5} M_\odot/\text{yr}$ . On the other hand the observed FWHM within the inner 160 pc of both  $H\alpha$  and  $[\text{N II}]$  and the equivalent width of the CaT lines are indicating the presence of an important population of red supergiants in the nucleus of NGC 6951 (Pérez et al. 2000). The current understanding of stellar winds is based on observations in the solar neighbourhood and so far there are no results concerning the possible effect of the intense radiation of the AGN on the wind structure. Thus stars in AGN might be very different from stars in the outer galaxy (Alexander & Netzer 1994; Alexander & Netzer 1997), and there are theories that the conditions in AGN are likely to enhance the mass-loss rate of irradiated stars near the center (Edwards 1980; Shull 1983; Voit & Shull 1988; Tout et al. 1989). While this radiation might not significantly increase the mass-loss rate (Voit & Shull 1988), Stecker et al. (1991) suggested a significant neutrino flux in AGN which may transform low-mass stars into red giants (MacDonald, Stanev, & Biermann 1991). Since we consider the the torus to be a consequence of two merging galaxies with central massive black holes, we not only expect stars to be brought into the center, but also big amounts of gas, and therefore the formation of young stars with high mass-loss rates. This is supported

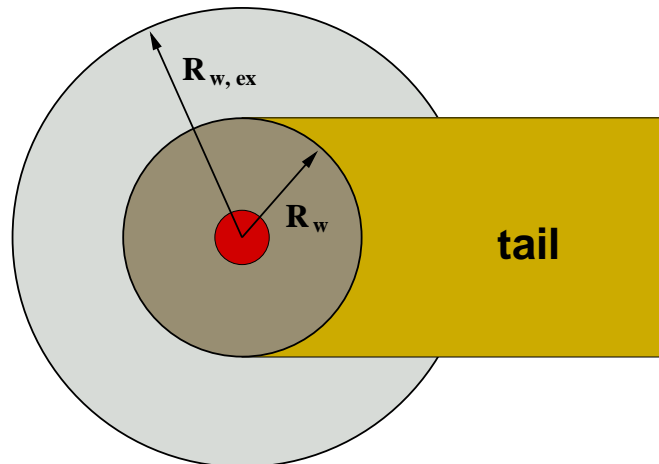


**Fig. 7.** This sketch illustrates how the radiation pressure of a strong source, located in a large distance  $d$  ( $d \gg R_{w,\text{ex}}$ ) left from the star, shapes the wind into a comet-like tail, pointing radially away from the source. The radius of the cross-section area of the wind is  $R_w$ , and  $R_{w,\text{ex}}$  denotes the radius of a freely expanding wind.

by Pérez et al. (2000), who find evidence that star formation occurs in bursts and continuously inwards to the nucleus from a 5 arcsec radius in NGC 6951, and Oliva et al. (1995), who investigated in red supergiants as starburst tracers in galactic nuclei. They find a large value of  $L_H/M$  in NGC 1068, confirming the presence of a decaying starburst in the central regions ( $R < 3''$ ). We will condense the previous arguments into the simple assumption, that the obscuring stars with strong winds amount to a fraction of 1% of the central cluster.

The radiation pressure of a bright central source limits the wind-radius in its extension and will shape it into an elongated tail, pointing radially away from the central source. This is illustrated for one star in Fig. 7. The large light-grey shaded circular area represents the freely expanding wind of the stars in its center. If now the radiation pressure is acting on this wind, it is limited to a smaller extension (dark-grey area) and shaped into comet-like tail. In this figure the central source is assumed to be left from the star in a large distance compared to the wind-radius.

Such bending of the wind in a tail by radiation pressure can be deduced from a crude and simple estimate. According to Mathis, Rumpl, & Nordsieck (1977), Graphite with its evaporation temperature  $T_{\text{evap}} \sim 1500$  K is the major contributor to the extinction of the radiation outside its evaporation radius  $r_{\text{evap}}$ . This corresponds to the distance from the center, where the absorption of the central UV radiation by dust grains equals the rate at which it is reradiated as thermal IR radiation, such that the equilibrium temperature is the evaporation temperature. The absorption efficiency of the grains in the IR is much smaller than in the optical/UV, so that the re-emission in the near IR (NIR) must be optically thin. Barvainis (1987) approximated the IR-absorption efficiency by a

powerlaw ( $Q_\nu \propto \nu^\gamma$ ) with the index in the range 1 to 2. This yields a spectrum with a considerably narrower bump at  $2\ \mu\text{m}$  than is observed (Sanders et al. 1989; Haas et al. 2000) and which corresponds to the optically thin emission peak of the hottest grains at a temperature  $T_{\text{gr}} \approx 1500\ \text{K}$ . Hence, any model which seeks to explain the NIR bump in terms of thermal dust emission requires a range in the grain temperature. This is naturally included in our model, since the heated dust will be in equilibrium at different temperatures at different distances from the central radiation source. For the grain temperature as function of the distance  $r$  to the center Barvainis (1987) obtained

$$T_{\text{gr}} = 1650 \left( \frac{L_{\text{uv},46}}{r_{\text{pc}}^2} \right)^{\frac{5}{28}} e^{-5\tau_{\text{uv}}/28}\ \text{K}, \quad (6)$$

with  $\tau_{\text{uv}}$  as the optical depth of dust in the UV and  $L_{\text{uv},46}$  being the central UV luminosity in units of  $10^{46}\ \text{erg/s}$ .  $r_{\text{pc}}$  is the distance normalized to 1 pc. Using  $T_{\text{evap}}$  for the grain temperature and solving this equation for  $r$  gives the evaporation radius

$$r_{\text{evap}} = 4.05 L_{\text{uv},46}^{1/2} T_{\text{evap},3}^{-14/5}\ \text{pc}, \quad (7)$$

where  $T_{\text{evap},3}$  denotes the evaporation temperature in units of 1000 K.

Assuming a star to be located inside  $r_{\text{evap}}$  where the Thomson cross-section  $\sigma_{\text{th}}$  applies, its wind extension can be calculated using the same Ansatz as for the Eddington limit, i.e. equating the force of the central radiation acting on the wind particles with the kinetic force of the wind,

$$\frac{L_{\text{uv}}\sigma_{\text{th}}}{4\pi r^2 c} = \frac{m_{\text{p}}v_{\text{w}}^2}{R_{\text{w}}}. \quad (8)$$

With typical values of red giants for the wind velocity  $v_{\text{w}}$  (Knapp & Morris 1985; Winters, Dominik, & Sedlmayr 1994; Hoefner et al. 1996) this equation can be solved for the extension of the wind,

$$R_{\text{w}} \approx 1.2 \times 10^{-3} \left( \frac{r}{2\ \text{pc}} \right)^2 \left( \frac{v_{\text{w}}}{10\ \frac{\text{km}}{\text{s}}} \right)^2 \left( \frac{L_{\text{uv}}}{10^{46}\ \frac{\text{erg}}{\text{s}}} \right)^{-1}\ \text{pc} \quad (9)$$

This is only a very rough estimate. In the following we are seeking for a more robust value of the wind radius, which is based on confirmed limits of observations. As discussed in Sect. 2, these tell us that the torus is optically thick and the covering factor of its constituents, the stars, is about one. Therefore the number density of obscuring stars, integrated along the radial extension of the torus, yields a surface density of the number of stars ( $\Sigma_{\text{os}}$ ) which has to equal the inverse of the cross-section area of the stellar winds, i.e.

$$\Sigma_{\text{os}} = \frac{1}{\pi R_{\text{w}}^2}. \quad (10)$$

In this equation  $R_{\text{w}}$  denotes the radius of the cross-section area of the stellar wind perpendicular to its radial extension. To calculate the surface density we employ the number density profile of the singular isothermal sphere that

we have already used in paper I ( $n \propto r^{-2}$ ), and which has not been much altered by the merging-process of the two BHs (Fig. 2). With  $n_0$  being the number density in the distance  $r_0 = 1\ \text{pc}$  we can write

$$n(r) = n_0 \left( \frac{r_0}{r} \right)^2. \quad (11)$$

Integrating this density from the inner to the outer radius of the torus ( $r_{\text{in}}$  and  $r_{\text{out}}$  respectively) gives the surface density:

$$\Sigma_{\text{os}} = \int_{r_{\text{in}}}^{r_{\text{out}}} n(r) dr = \frac{n_0 r_0^2}{r_{\text{in}}} \left( 1 - \frac{r_{\text{in}}}{r_{\text{out}}} \right) \quad (12)$$

In order to determine the number density  $n_0$ , we have to calculate the number of obscuring stars in the torus, which corresponds to the fraction 0.01 of the number of stars which are still bound to the binary after the merger,  $N_{\text{bn}}$ . Integrating the number density in Eq. (11) over the volume of the torus gives us the number of obscuring stars  $N_{\text{os}}$ :

$$\begin{aligned} N_{\text{os}} &= \int_0^{2\pi} d\phi \int_{\theta_{\text{trs}}}^{\pi-\theta_{\text{trs}}} \sin\theta d\theta \int_{r_{\text{in}}}^{r_{\text{out}}} n(r) r^2 dr \\ &= 4\pi \cos\theta_{\text{trs}} n_0 r_0^2 (r_{\text{out}} - r_{\text{in}}), \end{aligned} \quad (13)$$

where  $\theta_{\text{trs}}$  is the half-opening angle of the torus. Solving this equation for  $n_0$  and applying it to Eq. (12), the wind radius can be computed with the help of Eq. (10) to

$$R_{\text{w}} = \left( \frac{N_{\text{os}}}{4 \cos\theta_{\text{trs}} r_{\text{in}} r_{\text{out}}} \right)^{-\frac{1}{2}} \approx 1.8 \times 10^{-3}\ \text{pc}. \quad (14)$$

In the last step we used the values for the torus that we have found in paper I in case of the mass-ratio  $q = 1$ . These are 1 pc for the inner radius in agreement with the evaporation radius (Lawrence 1991) and the distance of the BHs, where the binary hardens (Milosavljević & Merritt 2001). The density drops quickly with increasing radius and so we choose 5 pc for the outer radius. The half-opening angle is about  $60^\circ$  (see Fig. 5) and for the bound stars we used  $N_{\text{bn}} = 3 \times 10^8$ , with  $N_{\text{os}} = 0.01 N_{\text{bn}}$ , what is a little more than the minimum of stars required to allow the BHs to merge ( $2.3 \times 10^8$ ). The wind radius computed in Eq. (14) is in very good agreement with our crude estimate in Eq. (9) and thus confirms the assumptions we made to obtain it.

Such a wind has to be optically thick ( $N_{\text{H}} \simeq 10^{24}\ \text{cm}^{-2}$ ) for all line of sights through its cross-section. We assume, that the density of such a tail, if projected along its radial extension, yields a constant surface density. Thus the mass in the wind can be estimated to be of order of

$$M_{\text{w}} = \pi R_{\text{w}}^2 N_{\text{H}} m_{\text{p}} \approx 8.4 \times 10^{-2}\ M_{\odot}. \quad (15)$$

The final picture of our model for the torus is illustrated (not to scale) in Fig. 8. The sum of the winds of the obscuring stars, shaped into elongated tails by the central radiation pressure, form a patchy, optically and

## Red Giants & their winds constituting a torus

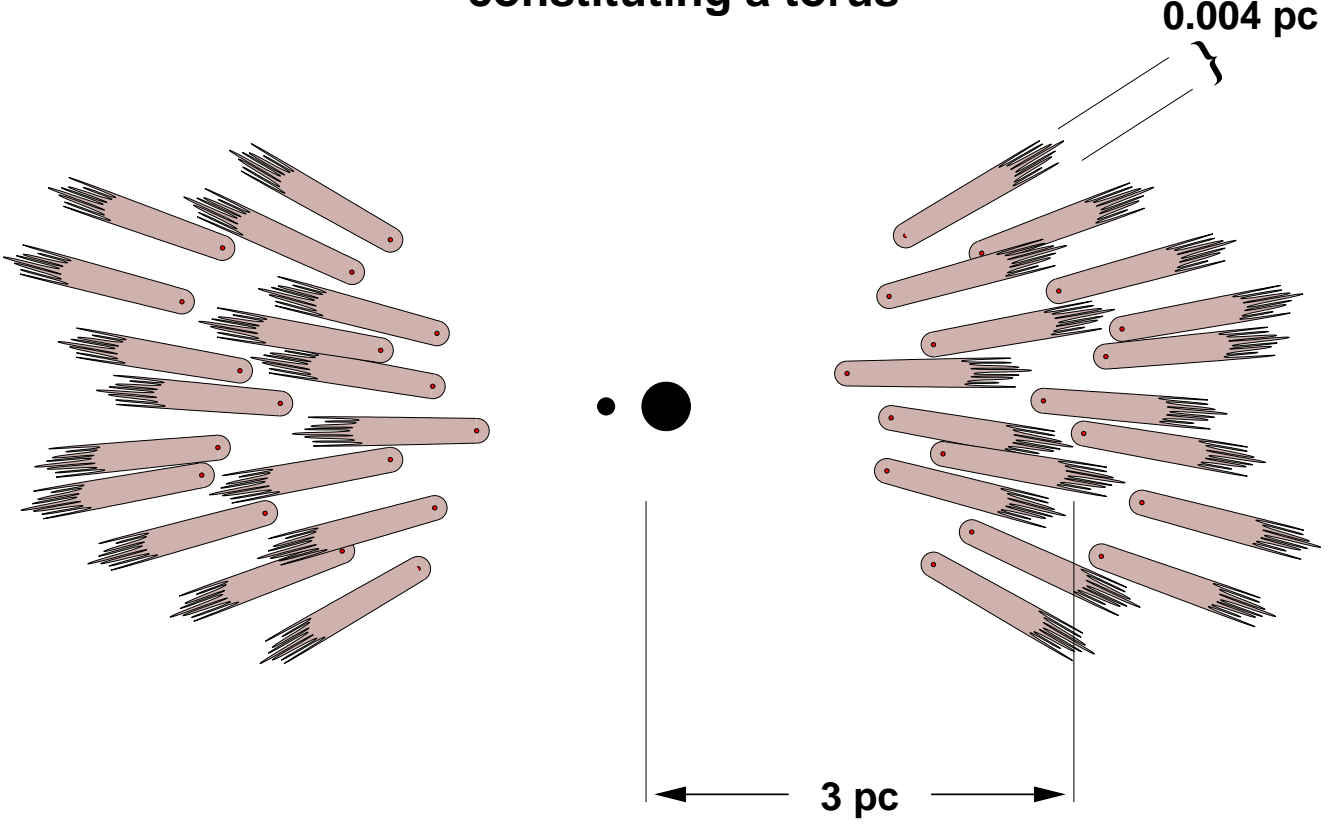


**Fig. 8.** This picture shows (not to scale) a sketch of the obscuring stars and their winds comprising a torus with the BBH in its center. In this cross-section through the torus, whose density peaks in about 3 pc distance, the obscuring stars are indicated by the small dots. They are surrounded by their winds, which are elongated by the central radiation into comet-like tails (shaded) with a lateral extent of about 0.004 pc. The central radiation source with the BBH is marked by the two BHs in the center. An observer with the LOS close to the edge of the torus might see the center through a gap directly, while the view of an observer with his LOS close to the equatorial plane of the BHs is probably blocked by the winds of at least one obscuring star.

geometrically thick torus. For an observer whose, line of sight (LOS) is aligned with such a wind, the nucleus is obscured and only radiation scattered into the LOS will be detected. Since the number density of the stars decreases for smaller inclination angles between the LOS and the symmetry axis of the torus, the probability to observe the nucleus not obscured, or only partially covered, through a gap in the torus, increases. Such gaps will be continuously open and closed because of the motion of the stars. Because Eq. (10) is satisfied, according to our prerequisite, the complete torus is optically thick on average.

With the number of obscuring stars and the mass in their winds we can estimate the order of magnitude of the dust-mass which is confined to the stellar winds outside the evaporation radius. The relation between the dust and gas mass is given by

$$m_d n_d = 1.4 Z_d m_p n_H, \quad (16)$$

where  $m_d$  and  $m_p$  denote the mass of a dust grain and the proton mass respectively. The number-densities are

accordingly given by  $n_d$  and  $n_H$  with  $Z_d$  as the dust-to-gas mass-ratio. Integrating over the volume of the wind yields  $M_d = 1.4 Z_d M_{\text{gas}}$ . This is substituted in  $M_w = M_d + M_{\text{gas}}$  and solved for the dust mass contained in the wind to result in

$$M_d = \frac{1.4 Z_d}{1 + 1.4 Z_d} M_w \approx 1.2 \times 10^{-4} M_{\odot}. \quad (17)$$

In the last expression we used the wind mass we have obtained before in equation (15) and for the dust-to-gas mass-ratio we used the value given by Hoefner et al. (1996),  $Z_d \approx 10^{-3}$ . Multiplying this dust mass with the number of obscuring stars needed to maintain a covering factor of 1 ( $N_{\text{os}} = 3 \times 10^6$ ) we get for the total dust mass contained in the wind of the obscuring stars

$$M_{d,\text{total}} = M_d N_{\text{os}} = 350 M_{\odot}. \quad (18)$$

This is about a factor of 10 more than the minimum values given by Sanders et al. (1989), which are required to fit the spectra. They obtain for the minimum of dust amounts

within spheres of the radii 1 pc and 10 pc the masses  $0.2 M_{\odot}$  and  $20 M_{\odot}$  respectively, using for the grains the parameters given in Mathis, Rumpl, & Nordsieck (1977) and Biermann & Harwit (1980). If all grains within the given radius are larger than  $\sim 1 \mu\text{m}$ , or are not directly exposed to UV radiation, the required dust mass is  $\sim 10$  times higher. Such shielding of the incident central radiation is actually expected in our model, since the stellar winds are shaped into elongated tails and the parts closer to the star will diminish the radiation which gets through to larger distances in the tail. With a covering factor of about 1 it is also likely that the wind of a star is covered by that of another one at smaller distances to the central source.

The picture which emerges from our simulations and the results is the following: If a BBH is surrounded by a stellar population of comparable mass, the stars which are ejected in violent interactions with the BHs are able to carry away enough angular momentum of the binary so that it hardens and gravitational radiation dominates the further shrinking of the distance of the BHs (paper I). Thus the binary finally merges on a timescale of  $10^7$  yr, spending most of the time in the range when the ejection of stars governs the process of hardening. On the other hand for the same number of initial stars there are enough left which are bound to the binary and form a torus-like distribution which peaks in about 3 pc distance. In this section we could show that the amount of obscuring stars in the remaining cluster is sufficiently large so that their winds achieve a total covering factor of about 1. Also their winds are strong enough such that they are optically thick. Thus the patchy torus as a total is geometrically as well as optically thick so that our model can indeed account for a dusty torus in the center of AGN, as is demanded by the unification model.

#### 4.1. Relativistic boosting

Within the solid angle of a relativistic jet, the radiation is boosted and so the flux density of the approaching radiation, seen under an angle  $\theta$  to the velocity of the moving source, scales as (Rybicki & Lightman 1979; Longair 1981)

$$S = D^{3-\alpha} S',$$

with  $\alpha$  being the spectral index and  $D$  the relativistic Doppler factor

$$D = \frac{1}{\gamma(1 - \beta \cos \theta)}.$$

The primed quantities refer to the comoving frame of the source. Thus, for an index  $\alpha \sim -1$ , the observed flux density depends on the Doppler factor to the power of four. Half of the radiation is emitted in a cone of half-opening angle  $\theta \simeq 1/\gamma$ , if  $\gamma \gg 1$ , and thus is strongly beamed. In this limit ( $\gamma \gg 1$ ) we have  $D \approx \gamma$  and the luminosity in the cone is a strongly increasing function of  $\gamma$ . If we assume the luminosity  $L$  to scale in the same way as  $S$

with  $\gamma$ , it increases very strongly in the beaming cone (i.e. by a factor of  $10^4$  for  $\gamma = 10$  and  $\alpha = -1$ ). Consequently, according to Eq. (9), the extension of the winds of the obscuring stars, exposed to the strong beamed radiation, is negligible and the covering factor in this region tends to zero. This means that within the beaming cone, and if the jet is precessing, within the cone of precession, the emission from the jet frees the polar cap regions from obscuring clouds, and therefore supports the toroidal structure of the central absorber.

#### 4.2. Lifetime of the torus

After the merger of the BBH is completed, the toroidal structure of the stellar distribution will not collapse and is stable (paper I). Therefore the torus will decay on timescales of the lifetime of its constituents, the obscuring stars (i.e. red super-giants and bloated super-giant stars) or has to be replenished with stars from outside. Since after the merger there is no torque anymore acting on the stars, the stars fed to the torus from larger distances would have to be accreted in an axi-symmetric way in order to maintain the torus-like shape of the circum-nuclear stellar distribution. The jet-outflow probably helps to keep the polar-cap regions free from stars. But it is expected, that the rate of stars accreted to the torus will decrease with time, as the outer regions, stirred up by the merger, will relax with time.

Thus, unless the required number of obscuring stars is not maintained for a longer time by the evolution of the other stars in the cluster, the life-time of the torus will be of comparable order as the time needed by the BBH to merge from that distance between the two BHs, when a torus has been built due to the binary's torque acting on the stars already in the more early stages of the merger. In paper I we obtained for the time scale of the merger about  $10^7$  yr, once the binary had become hard, with the BHs in  $\sim 1$  pc distance from each other.

In the next sections we present implications and predictions of the proposed model.

### 5. Jet-flip due to spin-flip of the primary BH

As we have already mentioned in paper I, we expect the merger of two galaxies of comparable size to result in a galaxy of early type, i.e. of elliptical shape. The spiral structure the parent galaxies might have had, will not survive such an event. On the other hand, radio-loud AGN so far have not been found in spiral host-galaxies, what suggests radio-loud galaxies to be the product of one or more major mergers. Since observations show that spectra from AGN in the range from IR to X-rays, dominated by emission from an accretion disk, are basically the same (Sanders et al. 1989), Wilson & Colbert (1995) argue that the distinction between radio-loud and radio-quiet AGN is due to the different spins of the central supermassive BHs. They propose radio-loud objects to harbour a fast spinning super-massive BH as result of a recent major merger,

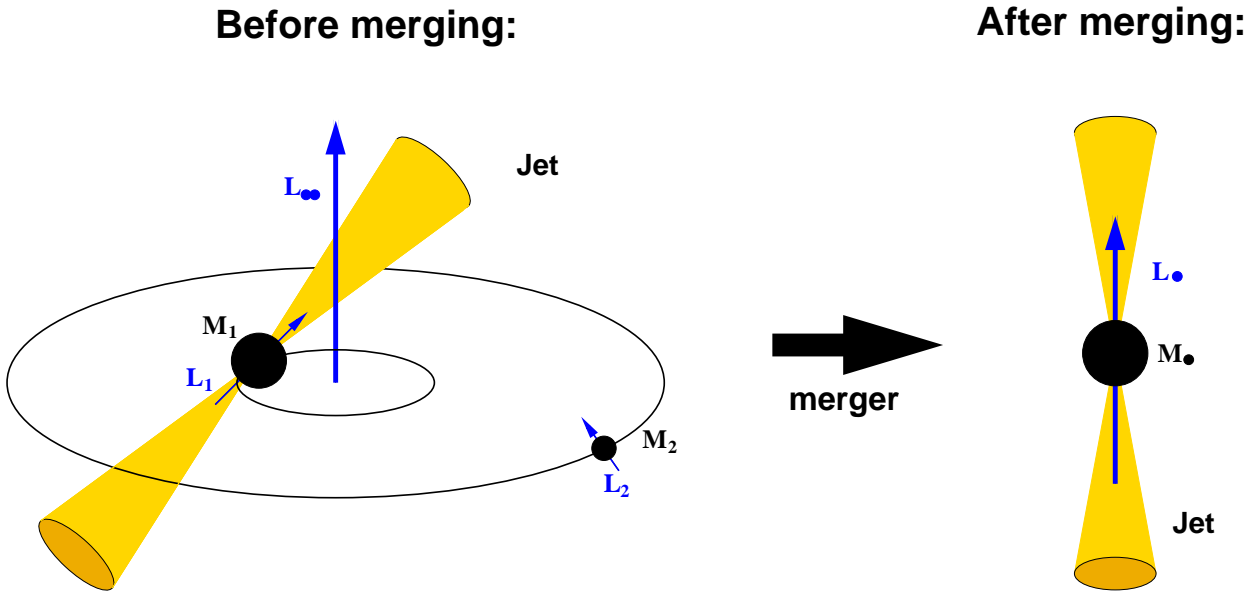


**Fig. 9.** This figure illustrates the change of the direction of the spin of the BH, induced by the merger of 2 massive BHs, and consequently the change of the direction of the jet. The left panel shows the situation before the merger, when the jet is aligned with the individual spin of the primary black hole of the binary system. The orbital angular momentum  $L_{\bullet\bullet}$  of the BBH and the spins of both BHs ( $L_1$  and  $L_2$ ) are randomly orientated to each other, since no direction of the plane of the merging galaxies is preferred relative to the spin of both the BHs in their centers. After the BHs coalesced (right panel), the different spins combine to that of the merged BH with a new direction ( $L_{\bullet}$ ). The jet emanating from the merged BH will be aligned with the new spin, which will be dominated by  $L_{\bullet\bullet}$ , and therefore has to jump from its orientation before the merger ( $L_1$ ) into this new direction.

with the assumption of non-rotating BHs in the parent galaxies. Since the time scales we obtained for the merging of the BHs are considerably smaller than a Hubble-time, this is in agreement with such a model.

But what happens, if one of the progenitor galaxies has a fast spinning BH in its center with a powerful radio-jet aligned with its spin? The situation before such BHs merge is depicted in the left panel of Fig. 9. The spins of both BHs, with that of  $M_2$  assumed to be negligible ( $L_2 \ll L_1$ ), and the orbital angular momentum of the BBH are randomly oriented to each other, because the merger of the two galaxies does not proceed in a favoured plane relative to the planes of the galaxies. For the spin of the primary BH,  $L_1$ , we adopt a value being sufficiently large to power a strong radio-jet according to the spin-paradigm. The maximum value is given by  $M_1 c R_g = GM_1^2/c$ , with  $R_g$  being the gravitational radius. For the orbital angular momentum we have  $L_{\bullet\bullet} = M_1 \sqrt{GM_1 a} / \sqrt{q(1+q)}$ , where  $q = M_1/M_2 \geq 1$  is the mass-ratio of both BHs and  $a$  is the semi-major axis. Thus we get for the ratio of these two angular momenta

$$\frac{L_{\bullet\bullet}}{L_1} = \frac{1}{\sqrt{q(1+q)}} \sqrt{\frac{a}{R_g}}. \quad (19)$$

It is a very interesting question now, what actually dominates the final spin of the merged black hole,  $L_{\bullet}$ . When the distance of both BHs has shrunk to about the last stable orbit ( $R_{ls} = 6R_g$ ) due to the emission of gravitational radiation, general relativistic effects become very important.

In this distance the orbital angular momentum dominates over the maximum possible spin of  $M_1$ , up to a mass-ratio of  $q = 2$ . This is actually a conservative limit since we neglected the last stable orbit of  $M_2$ . After further shrinking, when the BHs eventually merge, the final spin of the merged BH might be dominated by  $L_{\bullet\bullet}$  rather than  $L_1$ , with the merged black hole  $M_{\bullet}$  spinning close to its maximum value  $L_{\bullet} = GM_{\bullet}^2/c$ . This situation is shown in the right panel of Fig. 9. A new powerful radio-jet is emanating from the center aligned with the BH's spin which is pointing in the direction of  $L_{\bullet\bullet}$ , and therefore parallel to the symmetry-axis of the torus. This means that the jet is bending into a new direction, with the angle being enclosed by the old and new jet-axes corresponding to that between  $L_1$  and  $L_{\bullet\bullet}$  and thus it can assume any value. After the merger the old jet is not fed anymore from the center and its lobes will slowly fade away, while the new jet is digging its way through the ambient medium and the polar caps of the torus.

This might be the explanation for some of the most peculiar objects seen on the sky, the X-shaped radio-galaxies. They show a secondary, presently non-active pair of lobes, which is larger than and sometimes almost perpendicular to the presently active pair of lobes (Parma, Ekers, & Fanti 1985; Rottmann, Dennet-Thorpe, & Klein 1998), which we interpret in this picture as the new jet. This scenario is also in agreement with the involved time scales of some  $10^7$  yr for the merger and  $\sim 6 \times 10^7$  yr in B2 0828+32 for

the spectral aging of the secondary lobes (priv. comm. H. Rottmann).

Such a major merger will also increase the accretion-rate onto the BH which might be in favour of the arguments of Meier (2001), who suggests an association of jet production with geometrically thick accretion flows and BH rotation.

For larger values of  $q$  than 2 the possible influence of  $L_{\bullet\bullet}$  on the final BH spin is decreasing, and therefore also the bending of the jet into a new direction will have a decreasing amplitude. Thus we do not expect a jump of the jet in minor mergers where  $M_2 \ll M_1$  and therefore  $L_{\bullet\bullet} \ll L_1$  (see Eq. (19)) and ascribe the phenomenon of X-shaped radio-galaxies to recent major mergers, where one of the progenitors already had a powerful radio-jet. If radio strength is correlated with the spin of the BH, then the observations imply that a BH merger of spinning black holes leaves the ratio of spin to mass  $J/M$  large.

Before the two BHs finally coalesce, the surrounding patchy torus will have emerged on time scales of some  $10^7$  yr (paper I) in the plane of the merger, with its symmetry axis pointing along the binary's angular momentum. As long as the semimajor axis of the BBH is much larger than the last stable orbit of  $M_1$ , the old jet of the primary AGN is unaffected by  $M_2$  and still fed, as long as the feeding mechanism from the accretion disk is not interrupted. Because the orientation of this jet is not correlated with that of the torus, it might flow into the solid angle covered by the torus, where it will interact with stellar winds and ISM in between. After the BHs coalesced, the old jet will not be fed anymore, and the young post-merger jet is digging its way through the polar cap region of the torus, flowing along its symmetry axis. So both jets, the old and new, are interacting on sub-kpc scales with the ambient clumpy medium producing strong radio emission. This might be the cause of the so called Compact Symmetric Objects (CSO), which is a class of powerful radio sources consisting of high unbeamed luminosity radio emission regions separated by less than 1 kpc and situated symmetrically about the center of activity (Phillips & Mutel 1982; Wilkinson et al. 1994). It is thought that the high-brightness regions are due to hot spots and mini-lobes, which are created by the termination of jets streaming out into opposite directions from the center, see Owsianik & Conway (1998) and references therein. Instantaneous speed variations of some components in the CSO 0710+439 are most simply explained by interactions with a dense cloud medium, while other components are rapidly advancing through an intercloud medium. The expansion velocities are all of order  $0.2 h^{-1}c$  and therefore the age of these sources is estimated to be a few thousand years, showing that they are young rapidly growing sources (Owsianik, Conway, & Polatidis 1998; Owsianik, Conway, & Polatidis 1999). It is concluded that CSOs are probably young extragalactic radio-sources which will evolve via Medium-size Symmetric Objects into Large-size Symmetric Objects such as lower luminosity FR II dou-

ble radio-sources (Fanti et al. 1995; Readhead et al. 1996; Owsianik & Conway 1998).

If the X-shaped radio galaxies are correctly explained with our proposed picture, the resulting gravitational wave pattern will strongly depend on the orientation of the three relevant spins and therefore on the re-orientation of the primary black hole. It experiences a spin-flip in this picture.

## 6. BAL QSOs – QSOs seen at intermediate inclination

The broad absorption line (BAL) quasars comprise about 10% of the optically selected quasars, see for example the review by Antonucci (2001b) and the article by Schmidt & Hines (1999). Since they are hard to find at optical wavelengths, their real fraction is thought to be in the range 20% – 30%. Moreover the BAL covering factor is thought to be much less than unity and consequently there must be many objects, if not all, being intrinsically the same as BAL quasars, but not classified as such if seen from other directions. The region which is responsible for the formation of the BAL partially absorbs the broad emission lines, and therefore it must be outside the BLR. Also the polarization in the broad emission lines is observed to be lower than the polarization in the absorption troughs of the BALs.

All these arguments fit well into the unification model, where the BAL quasars are quasars seen at intermediate inclination angles, with the line of sight grazing the surface of the obscuring dusty torus (Weymann et al. 1991; Voit, Weymann, & Korista 1993) and thus is supported by our model. Objects seen at lower inclinations are classified as quasars, and at inclinations smaller than the boosting angle as Blazars. For larger inclinations the line of sight will intersect with more absorbing material since it approaches the surface of the dusty and patchy torus, which does not have a sharp defined edge. Thus less of the BLR is seen directly and the fraction of scattered light as well as the polarization is increasing. In this scenario the region where the BALs are formed extends from the surface of the torus at about  $45^\circ$  to smaller angles, in the extreme up to the edge of the jet at  $\theta \sim 1/\gamma$ . With increasing inclination the view to the nucleus is increasingly blocked by the torus and the quasar will appear more reddened (IRAS QSO) and finally, seen edge on, becoming a QSO of Type 2 (ULIRG or FR II radio galaxy).

Inside the torus, with its inner edge close to the evaporation radius of dust ( $\sim 1$  pc) the heated matter will be accelerated and streams away from the nucleus through the gap between jet and torus either in form of clouds or as a wind. Here, above the surface where the density of the torus gradually decreases, the clouds are exposed to more intense radiation. Assuming the half opening angle of the torus to be  $\theta_{\text{trs}} = 45^\circ$ , the maximum covering factor of the BAL region which can be achieved is

$$C_{\text{BAL}} = \cos \theta_1 - \cos \theta_{\text{trs}} \approx 0.3$$

for  $\theta_1 = 0$ . If we identify the smallest possible value for  $\theta_1$  with the beaming angle of the jet (i.e.  $\theta_1 = \theta_{\text{jet}} = 1/\gamma$ ) we obtain for the covering factor  $C_{\text{BAL}} = 0.27$  and  $0.29$  if  $\gamma = 5$  and  $10$  respectively. This is in good agreement with the assumption that the fraction of BAL QSOs of  $0.2$  to  $0.3$  represents the covering factor  $C_{\text{BAL}}$  in the same range (Weymann 1997).

From the *FIRST* survey Gregg et al. (2000) report the discovery of the quasar FIRST J101614.3+520916, whose optical spectrum shows BAL features and at the same time radio loud emission from lobes of classic FR II type. An inclination of the jet-axis to the LOS of more than  $40^\circ$  is deduced and the authors conclude that this quasar is in contradiction with the orientation model as explanation for BAL QSOs. Contrary to this conclusion we claim that these observations actually support the orientation model. According to the above numbers, BAL QSOs are seen at intermediate angles between the boosting angle of the jet and the half opening angle of the torus at about  $45^\circ$ . Thus the LOS to the core of J101614.3+520916 is grazing the surface of the patchy obscuring torus, whose constituting absorbers, the stellar winds, are increasing in number density towards the equatorial plane. At higher inclinations the torus would block the free view to the center completely and no BALs could be detected, so that this object would appear as a typical FR II quasar. This is also in agreement with BAL QSOs, that show large radio lobes, being so rare. For J101614.3+520916 Gregg et al. (2000) find that it has some properties in common with low-ionization BAL QSOs, as for example higher reddening. Schmidt & Hines (1999) find in their investigation BAL QSOs to be typically 2.4 times more polarized in the optical than QSOs. And among the BAL QSOs the subclass of low-ionization absorbers shows evidence to be stronger polarized than the other BAL QSOs. Also the low-ionization BAL QSOs show evidence to be reddened by dust (Sprayberry & Foltz 1992; Egami et al. 1996). Assuming that the same intrinsic power-law with index  $\Gamma \approx 1.8$ , which is consistent with the mean slope of radio quiet QSOs and has been derived for high-ionization BAL QSOs, applies to all BAL QSOs, Green et al. (2001) infer that the low-ionization BAL QSOs are enshrouded by an additional intrinsic column density of nearly  $10^{23-24} \text{ cm}^{-2}$ . Because of a decrease in polarization with increasing wavelengths in some of these objects, they are suggested to be seen edge-on with dust-scattering (Kartje 1995) and in which the scattered line of sight is less reddened. Therefore the low-ionization BAL QSOs have been proposed by Brotherton et al. (1997) as the most edge-on QSOs. In this line of argument Green et al. (2001) point out the possible link of these objects to ULIRGs, of which at least a fraction is believed to be edge-on seen QSOs, i.e. quasars of Type 2. Thus the BAL QSOs fit into the sequence in which a QSO appears as Blazar seen pole on and as the inclination angle increases as quasar, high-ionization BAL QSO, low-ionization BAL QSO and finally as ULIRG if seen edge-on.

In case of J101614.3+520916 Gregg et al. (2000) suggest that this quasar rather happens to be seen in a rare and short-lived state, showing both, BAL features and developed radio lobes at the same time. The core of J101614.3+520916 being a compact steep spectrum (CSS) or gigahertz-peaked spectrum (GPS) radio source then leads to their postulation that it is a rejuvenated quasar, possibly through merger. We do not exclude such evolutionary effects, but as shown above, we also expect a merger to seriously affect the jet, what should be detectable. And the question to be answered for the evolutionary/rejuvenated scenario is: What is the explanation then for the difference between the radio-quiet BAL and non-BAL quasars?

The earlier assumption, that BAL QSOs have the same underlying X-ray continuum just as normal QSOs, has been confirmed in some recent publications (Gallagher et al. 2001; Green et al. 2001; Gallagher et al. 2002). The *ASCA* observations by Gallagher et al. (2001) give evidence for X-ray absorption in sources showing UV absorption. After their correction of the observed X-ray spectra for intrinsic partial absorption with column densities in the range  $N_{\text{H}} = 10^{22-23} \text{ cm}^{-2}$ , a photon index and optical-to-X-ray spectral index in agreement with those of typical AGN of Type 1 is obtained. The variability of the BAL quasar PG 2112+059 between the *ROSAT* and *ASCA* observations on scales of 6 yr is related to changes in the absorber, either the ionization parameter, or the column density. When the absorbing clouds are moving through the line of sight as proposed by our model, the column density changes on the above observed time scales, and therefore further variations in the spectrum are expected (see Sect. 7).

Green et al. (2001) conducted a short-exposure survey of a sample of 10 bright BAL QSOs with *Chandra*. The simultaneous fit of the spectra of six BAL QSOs showed best results for an underlying power-law with spectral index  $\Gamma = 1.80 \pm 0.35$ , being consistent with the mean slope of radio quiet QSOs, which is partially covered by an intrinsic absorber with a column density  $N_{\text{H}} \sim 10^{22} \text{ cm}^{-2}$ . They find the low-ionization BAL QSOs to be weak in X-rays what could be explained by a substantially higher column density of the absorbers. As an alternative to the orientation hypothesis they indicate evolutionary effects, though their results do not support this idea.

In their investigation in X-ray spectroscopy of BAL QSOs Gallagher et al. (2002) also find typical column densities of  $N_{\text{H}} \sim 10^{23}$  in agreement with our suggestion of stellar winds being the absorbers. For five of eight observed sources a partial-covering absorber provides a significantly better fit of the flux than a neutral absorber. Due to the patchy nature of the torus, we propose partial covering absorption plus scattering in order to fit the spectra of BAL QSOs.

## 7. Application to Type-varying Objects

With such a model for the obscuring patchy torus, as developed in this paper, one observable consequence is a possible variation of the absorption properties, i.e. the column density. This has been mentioned before in Sect. 6 as explanation for the observed changes in the absorber properties of the BAL QSO PG 2112+059 on time scales of 6 yr.

When an obscuring cloud or stellar wind of the torus is moving into (out of) the line of sight of the observer to the radiation source, the column density will drastically increase (decrease) and the source will gradually appear much weaker (brighter) in luminosity. For our chosen AGN with  $M_1 = 10^8 M_\odot$  we obtained the circumnuclear torus to be located in a distance of a few parsecs to the center. The radius of the wind of the obscuring stars we computed to be of order of 0.002 pc. For a star moving on Keplerian orbits in the potential of such a BH, the velocity is  $v = \sqrt{GM_1/r}$ . Therefore the time required for the star's wind to move along its diameter from one edge to the other through the line of sight is

$$t_{\text{var}} = 2 \frac{R_w}{v} \approx 10 \frac{R_w}{0.002 \text{ pc}} \left( \frac{r}{3 \text{ pc}} \right)^{\frac{1}{2}} \left( \frac{M_1}{10^8 M_\odot} \right)^{-\frac{1}{2}} \text{ yr}. \quad (20)$$

Consequently variations of the column density and the luminosity are expected to happen on scales of a decade. Since the density of stars is enhanced towards the equatorial plane of the torus it is likely that there are more than one stars in the line of sight and thus a transition from optically thick to thin or vice versa will be a rare event if the torus is seen edge on. But if the line of sight grazes the surface the torus the chance to observe such a transition will be higher. And indeed there are a couple of observations which fit well to this interpretation.

Before comparing the above computed time scale for a transformation from Type 1  $\rightarrow$  2 with observations, we want to scale it just in a simple way with the mass of the central BH.

Assuming the luminosity to be proportional to the eddington,  $L_{\text{edd}} = 4\pi GcM_1 m_p / \sigma_{\text{Th}}$ , we have  $L \propto M_1$ . Thus with Eq. (9) the wind radius scales as

$$R_w \propto \frac{r^2}{L} \propto \frac{r^2}{M_1}.$$

Together with  $v_{\text{kep}} \propto \sqrt{M_1/r}$  the dependency of the time on mass and radius is:

$$t_{\text{var}} \propto \frac{r^{5/2}}{M_1^{3/2}}.$$

There are now at least two possibilities for the choice of the inner radius of the torus:

(1) The evaporation radius, for which we have  $r_{\text{evap}} \propto L^{1/2} \propto M_1^{1/2}$  (see Eq. (7)). Thus we obtain the dependency

$$t_{\text{var}} \propto M_1^{-1/4}, \quad (21)$$

what means that the time required for a cloud passing through the line of sight is decreasing with increasing mass of the central BH.

(2) Another choice for the radius of the torus is the distance of the BHs, when the binary is hard, since the simulation showed that this coincides within a factor of a few with the radius of the torus (paper I). According to Milosavljević & Merritt (2001) the binary becomes hard at a semi-major axis  $a_h = GM_{\bullet\bullet}/8\sigma^2$ . Using the relation

$$M_{\bullet} = 1.3 \times 10^8 M_\odot \left( \frac{\sigma}{200 \text{ km/s}} \right)^\alpha,$$

with  $\alpha = 4.72(\pm 0.36)$  (found by Merritt & Ferrarese (2001a, 2001b)) we get

$$t_{\text{var}} \propto M_1^{(\alpha-5)/\alpha} \approx M_1^{-8/135}. \quad (22)$$

Again there is a negative exponent, albeit small, so that  $t$  is decreasing with increasing  $M_1$ , as for  $r = r_{\text{evap}}$ .

To obtain a dependency so that  $t$  is decreasing with  $M_1$ , the radius of the torus has to fulfil the dependency  $r \propto M_1^\eta$ , with  $\eta > 3/5$ . Since the exponents in the time-mass relation are much smaller than 1 for both choices of the inner radius of the torus, the transition-time does not depend strongly on the mass of the central BH, and is almost constant on orders of 10 yr.

In the following we will show that the patchy torus with the possibility of variations in the obscuring column density and thus of the transition of the type of AGN is in good agreement with the observations.

*NGC 7582*: Based on observations in the X-ray band of the Seyfert 2 galaxy NGC 7582 (Maccacaro & Perola 1981; Mushotzky 1982; Reichert et al. 1985; Turner & Pounds 1989; Warwick et al. 1993) it has been suggested that the central X-rays are obscured by matter with a column density of  $N_{\text{H}} > 10^{23} \text{ cm}^{-2}$ . In *ASCA* data Xue et al. (1998) find variabilities of hard X-rays on short time scales which are in agreement with the nuclear emission of NGC 7582 being similar to that of Type 1 Seyferts. Their best fit model consists of an absorbed powerlaw with a spectral index of about 1.3–1.6, a scattered component and a thermal component which contributes at most about 10–20% of the flux at 1 keV and is ascribed to starburst emission. Compared to spectral indices of other Seyfert 2s ( $\Gamma \approx 2$ ) the X-ray spectrum in NGC 7582 is rather hard. The flattening of the spectrum can be explained with the ‘‘Dual-Absorber’’ model in which the continuum is completely covered by a torus of nonuniform density. With an additional column density of  $N_{\text{H}} \simeq 6.3 \times 10^{23} \text{ cm}^{-2}$  Xue et al. (1998) obtain a good fit to the data with a steep powerlaw component, which is consistent with the observed equivalent width of the iron  $K\alpha$  line. This best fit model is in agreement with the unification scheme and a torus is blocking the direct sight to the center.

On the long time range between the two *ASCA* observations from November 1994 and 1996 the spectral index does not show a significant variation while the column density of the absorber, the putative torus, seems

to have increased by  $\sim 44\%$ . These results, found by Xue et al. (1998), confirm previous observations with *Ginga* by Warwick et al. (1993), who detect a significant increase of the column density to  $\sim 4.6 \times 10^{23} \text{ cm}^{-2}$  by a factor of about 3 compared to the *EXOSAT* observations 4 yr before. Thus over a time-range of about 13 yr from the *EXOSAT* to the *ASCA* observations in 1996 the column density has increased.

Later, during the observations from July 11 to October 21 in 1998, Aretxaga et al. (1999) detect variations in the range 340 – 750 nm. First the continuum flux at 340 nm decreases by 50% between July 11 and October 6, and afterwards increases again by 30% till October 21. They examined three scenarios that potentially could explain such transitions: The central black hole captured a star which is disrupted. This would need the idea of an obscuring dusty torus to be dropped, since it would block otherwise the central optical emission. Another possibility would be a change of reddening in the surrounding torus as suggested by the unification scheme with a patchy torus. But the time scales involved are too short in order to be explained by the patchy absorbers within the torus moving through the line of sight. Another alternative for the transition might be located outside the torus in a compact circum-nuclear starburst region, due to the radiative onset of a Type II supernova explosion.

One year later Turner et al. (2000) presented *BeppoSAX* observations of NGC 7582, made during November 1998. They find the nuclear X-ray flux to be unrelated to the gradual decline in optical flux, detected since the high state in July of that year. The hard X-ray component, peaking close to 20 keV, shows rapid variability, in correlation with the 5 – 10 and 13 – 60 keV bands, but the 0.5 – 2 keV flux does not show significant variations within the *BeppoSAX* observation. In both X-ray bands, hard and soft, the nucleus clearly has brightened since the 1994 *ASCA* observation. Turner et al. (2000) interpret the increase in soft X-rays to be consistent with the appearance of holes in the full screen which allow  $\lesssim 1\%$  of the nuclear flux to escape, and to produce some clear line of sight to the BLR. The authors also find evidence for larger absorption at the *BeppoSAX* epoch. The 2 – 100 keV spectrum is well fitted by a powerlaw with index  $\Gamma \approx 1.95$  and attenuation due to a dual absorber. The “thick absorber” covers 60% of the nucleus, corresponding to a half-opening angle of a torus of about  $53^\circ$ , and has a column density of  $1.6 \times 10^{24} \text{ cm}^{-2}$ . The entire nucleus is additionally covered by a “full screen” absorber with column density  $1.4 \times 10^{23} \text{ cm}^{-2}$ , which has increased by  $\Delta N_{\text{H}} \simeq 7 \times 10^{22} \text{ cm}^{-2}$  since the 1994 *ASCA* observation.

Thus the column density of NGC 7582 has increased over a timescale of about 15 yr from the *EXOSAT* to the *BeppoSAX* observation. This is in very good agreement with the time scales for major variations in the column density that we have computed above, and therefore strongly supports the idea, that the torus indeed is comprised of many individual absorbers, i.e. stellar winds, moving through the line of sight.

*NGC 2992*: Another such object which has been observed to change its type is NGC 2992, which is classified as a Seyfert 1.9 galaxy. Fitting the *ASCA* data from the observation in 1994 in the range 0.5 – 5 keV, Weaver et al. (1996) obtained for a uniformly absorbed power law the parameters  $\Gamma \approx 1.23$  and  $N_{\text{H}} \approx 1.8 \times 10^{21} \text{ cm}^{-2}$ , which they find to be much flatter than previous results from *HEAO* (Mushotzky 1982; Singh, Garmire, & Nousek 1985), *Einstein* (Halpern 1982; Turner et al. 1991) *EXOSAT* (Turner & Pounds 1989) and *Ginga* (Nandra & Pounds 1994) observations. A clear trend is detected, that the index depends on the used bandpass, implying a more complex intrinsic spectrum, and that the spectrum itself retains a constant shape in spite of different results obtained with different telescopes. Employing a partial covering model to fit the *ASCA* data, which are suggested to be biased towards a flat slope, the spectrum is equally well fitted with an index  $\Gamma = 1.7$  and a column density of  $\sim 10^{22} \text{ cm}^{-2}$  (Weaver et al. 1996). In their analyses of the Fe K $\alpha$  line these authors conclude that its equivalent width is most likely due to a time lag in the response of the line flux to the continuum flux. Comparing the time scales on which the continuum decreases by a factor of 3 with that of the Fe K flux to decrease by the same factor allows them to roughly estimate the time lag for the reprocessed X-rays. This turns out to be about 10 yr, which puts the reprocessor in a distance  $\sim 3.2 \text{ pc}$ , so that the reprocessor can be identified with the torus. This distance is in very good agreement with the 3 pc that we obtained for the distance of the maximum of the torus’ density. Optical observations suggest a half-opening angle of the ionization cone of  $\sim 65^\circ$  (Tsvetanov, Dopita, & Allen 1995), which restricts the covering factor of the torus to  $\sim 0.42$ . Weaver et al. (1996) used this value to compute a column density of  $\sim 3 \times 10^{23} \text{ cm}^{-2}$  in order to produce the Fe K line.

Comparison by Weaver et al. (1996) of the 2 – 10 keV X-ray band of *ASCA* observations in 1994 with previous observations show a steady decline on a range of 16 yr by a factor of about 20. During this time the data suggest the spectrum to be constant in shape. If the intrinsic flux also stays constant, it is likely that the line of sight is intersecting with an absorber with a column density increasing during the 16 yr before the *ASCA* observation, and thus is in favour of the patchy torus being comprised of stars and their winds.

Gilli et al. (2000) report about two subsequent observations of NGC 2992 with *BeppoSAX* in 1997 and 1998, both being well fitted by a power law with index  $\Gamma \simeq 1.7$ , which is absorbed by a column density of  $N_{\text{H}} \simeq 10^{22} \text{ cm}^{-2}$ , and shows a prominent Fe K $\alpha$  line. While the 2 – 10 keV flux measured in 1997 shows a modest increase compared to the *ASCA* flux from 1994, the flux detected in 1998 is almost at the same level as in 1978, and is stronger by a factor of about 12 compared to the flux in 1997. The authors interpret these long-time flux variations in terms of different phases of the rebuilding of an accretion disk, which is estimated to last 1–5 years. Short-time variabilities in flux, like that known in Seyfert 1 galaxies, are ob-

served in the 1998 data of *BeppoSAX*, but not in the low states of 1994 and 1997. This can be explained naturally in terms of the patchy torus: In the low state an optically thick cloud or stellar wind blocks the line of sight to the center, and thus to the source continuum and its variations on short time scales. And in the high state the line of sight penetrates the torus through a gap, and the source flux and its variation is directly visible.

In the AGN scenario with an accretion disk model Gilli et al. (2000) obtain for the *BeppoSAX* data from 1998 a relative normalization between the direct and reflected continuum  $R = 0.12$ , which disagrees with the value 1, that is predicted for an isotropic source irradiating a plane-parallel semi-infinite disk, and by the equivalent width of the line. The authors can solve this problem by assuming that the source is observed through a dual absorber with a column density in the range  $10^{22-23} \text{ cm}^{-2}$ , which, together with a canonical power law of index  $\Gamma \sim 1.9$  and a reflection component, resembles a power law with flatter index 1.7.

For the interpretation of the observations of NGC 2992 we prefer the patchy torus with its individual stellar winds moving in and out of the line of sight to the rebuilding accretion disk as reason for the decline and subsequent increase of the flux over a total of 20 yr. According to Weaver et al. (1996) the spectrum seems to have been constant between 1978 and 1994, and Gilli et al. (2000) find it in 1998 also to be very similar to that in 1978. This is easily explained within our model, since the reason for flux changes is the change in column density of the absorber, while the source continuum can stay constant. But it might be difficult to be explained by a source continuum which maintains its spectral shape during the process of rebuilding the accretion disk. Also the time scales involved for the slow destruction or fading of the disk on scales of about 16 yr compared to the rebuilding within 1 to 5 years could be problematic to interpret in terms of the disk. For a patchy absorber it is possible that more than one cloud or stellar wind happen to block the line of sight, and depending on their individual velocities and directions in which they move, it is possible that the decrease and increase of the central flux proceeds on different time scales.

If the flux changes are really caused by rebuilding an accretion disk, also the parts of the spectrum which are emitted isotropically should show variations, maybe with certain time-lags though. For instance the IR is thought to be radiated isotropically and within the patchy torus would stay constant, independent on changes of the absorber which are due to movements of its constituents. Gilli et al. (2000) find some variations in IR flux, but on shorter time scales than the rebuilding of the disk requires. So these variations might be caused by other events on shorter time scales, maybe by a starburst region outside the torus. We expect variations in the IR as a consequence to variations in the accretion disk to occur on longer time scales and to show a certain time lag relative to primary disk continuum, since it needs some time to be reprocessed by the outer matter, i.e. by the torus.

*NGC 4051*: The low-luminosity Seyfert 1 galaxy NGC 4051 is another galaxy whose luminosity has been observed by Guainazzi et al. (1998) to decrease by a factor of about 20 in the range 2 – 10 keV. While this flux has been almost constant for more than 10 yr till the *RXTE* observations by Uttley et al. (1998) it is measured to be 20 times fainter 1.5 yr later with *BeppoSAX* in 1998 by Guainazzi et al. (1998). Their best fit model is a bare reflection model with an additional Gaussian component that accounts for the iron  $K\alpha$  peak. This leads the authors to interpret the drop in luminosity in terms of a switched off nuclear source with only the Compton reflection component being detected as an echo of past activity. A model with a strongly absorbed ( $N_{\text{H}} \sim 3 \times 10^{24} \text{ cm}^{-2}$ ) power law with index  $\Gamma = 1.9$  and reflection of a plane-parallel infinite slab yields a significantly worse fit which underestimates the flux in the range of 13 – 50 keV. Still, a column density of at least  $1.4 \times 10^{26} \text{ cm}^{-2}$  being responsible for the fading due to stronger absorption instead of the primary continuum being switched off can not be ruled out. In Fig. 3 of Guainazzi et al. (1998) the best fitting models for the 1995 *ASCA* and 1998 *BeppoSAX* data are displayed. It can be seen that the power law used for the *ASCA* data, if extrapolated to energies more than 30 keV, approximates the fit of the *BeppoSAX* data, which stay a little below such an extrapolation. This should be in favour of a heavily obscured AGN. Also the reflection-dominated X-ray spectrum closely resembles those observed in Compton-thick Seyfert 2 galaxies (Iwasawa & Comastri 1998; Iwasawa, Fabian, & Matt 1997; Matt et al. 1996; Matt et al. 1997), where the nucleus is likely to be completely covered rather than switched off. But the time scale of  $\sim 1.5$  yr for the decrease of the luminosity by a factor of 20 might be too short to be accounted for by a cloud in the patchy torus moving in the line of sight. Since both models predict a reflection dominated spectrum it will be not easy to distinguish between them.

*NGC 1365*: Risaliti, Maiolino, & Bassani (2000) report on *BeppoSAX* observations in August 1997 of the Seyfert 1.8 galaxy NGC 1365. They detect a flux in the 2 – 10 keV band which is 6 times brighter than that measured almost 3 years before by *ASCA*. The spectrum is well represented by a power law with index  $\Gamma = 1.93$  (typical for Seyfert 1 galaxies), a photoelectric cut-off which corresponds to column density of cold absorbing material ( $N_{\text{H}} \sim 4 \times 10^{23} \text{ cm}^{-2}$ ), and a second power law, which fits the soft excess that is ascribed to more extended components, like starbursts or hot gas in the NLR. Because of the high reflection efficiency, which is deduced from comparison of the *ASCA* and *BeppoSAX* observations, a much higher column density for the reflector is required than that measured in absorption. Therefore the authors conclude that the circumnuclear medium is strongly inhomogeneous, i.e. the torus contains Compton thick clouds ( $N_{\text{H}} > 10^{24} \text{ cm}^{-2}$ , patchy torus) or is stratified with the maximum density in the equatorial plane. The flux variation between both observations is explained either by an intrinsically lower emission during the *ASCA* obser-

vation, or by a compton thick cloud passing through our line of sight and which obscured the nucleus during the 1994 *ASCA* observation, making that spectrum reflection dominated. This latter explanation is in exact agreement with the patchy torus.

*NGC 3227*: For the Seyfert galaxy NGC 3227 George et al. (1998) compared the data from *ASCA* observations in 1993 and 1995 and *ROSAT* observations in 1993. Their best-fit model for the spectrum consists of an underlying power law which is absorbed by two screens of neutral material, one of which is located within our galaxy, and a screen of ionized material. The variations of the spectra during the observations in 1993 and 1995 are ascribed to variations in the underlying spectral index. For the observations in 1995 the authors find evidence that about 13% of the observed continuum is attenuated by the ionized absorber with a column density of  $N_{\text{H}} \sim 3 \times 10^{22} \text{ cm}^{-2}$ . They find this to be consistent with either only a fraction of the cylinder of sight to be covered by the absorber (clouds) or the whole cylinder of sight to be covered by the absorber, but with a fraction of the continuum escaping through another light path. Actually both these possibilities can be explained with a patchy torus, consisting of lots of absorbing clouds, the stellar winds. They might cover the complete cylinder of sight, but since the covering factor of the whole torus they comprise, as seen from the central source, is about 1, there will be gaps in this torus. Through these gaps a fraction of the central source can escape and might be scattered into the line of sight. On the other hand the line of sight might go through such a gap directly, or is partially covered by a cloud which is just moving into or out this cylinder. George et al. (1998) show that the column density of the ionized absorber increased by about an order of magnitude, i.e. from  $N_{\text{H}} \sim 3 \times 10^{21} \text{ cm}^{-2}$  in 1993 to  $N_{\text{H}} \sim 3 \times 10^{22} \text{ cm}^{-2}$  in 1995. They think this to be most naturally explained by a cloud of material moving into the cylinder of sight, supporting our idea that the obscuring torus is patchy and the patches are actually stellar winds.

In this section we showed that our model of an obscuring torus, being comprised of stellar winds, which are shaped into elongated tails by the central radiation pressure, passed an important test. A covering factor of the torus of about unity means that not necessarily all lines of sight through the torus to the central radiation source are covered and that due to the motions of the stars in the torus under the influence of the central BHs such gaps will form and will be closed continuously. Consequently the column density along a certain line of sight will change with time on scales of about 10 yr according to our model. The above observations of changes in the column density and the involved time scales are in very good agreement with these predictions.

## 8. Influence and implications of the binary's mass-ratio

Our simulations in paper I showed that for a decreasing mass-ratio of the BHs ( $q = M_1/M_2 \geq 1$ , with  $M_1 = 10^8 M_{\odot} = \text{const.}$ ) the fraction of the ejected stars is increasing. But to extract the bigger amount of angular momentum from a more massive binary ( $L_{\bullet} = \sqrt{GM_1^3 a} / \sqrt{q(q+1)}$ ), the increased fraction of ejected stars is not sufficient, so that the star cluster has to be more massive in order to absorb the binary's angular momentum and to enable the BHs to coalesce. Therefore the amount of bound stars has to increase with the mass  $M_2$  of the secondary BH, and so the torus becomes more massive.

As we have pointed out in the discussion of the influence of the mass-ratio, the inner regions become increasingly unstable for more massive secondary BHs, so that at the inner edge of the torus the stars are moving on almost circular orbits to avoid violent interactions with the binary. For sufficiently small mass-ratios a more sharp defined torus forms during the late stages of the merger, while for young mergers and mergers with large mass-ratios a more diffuse and shell-like density distribution of the stars is maintained. This is clearly visible in Figs. 2 and 14 of paper I, which also show a larger half-opening angle of the torus in the range  $50^\circ$  to  $60^\circ$  for  $q = 1$  (i.e.  $M_2 = M_1$ ) compared to about  $45^\circ$  for  $q = 10$ . This is due to the stronger torque that is exerted by the binary with smaller  $q$  on stars in the polar cap region, and therefore less orbits are passing through this region.

In major mergers we also expect the accretion rate on the central BH to be much higher and thus these mergers to be much more luminous than minor ones. This is in agreement with the idea that the opening angle depends on the luminosity, being larger for the more luminous AGN. Consequently the radiation pressure acting on the torus and its stars is less in minor mergers, and according to Eq. (9) the radius of the stellar winds can extend to much larger radii, not being stretched into elongated tails. Hence the column density along the LOS to the center is diminished and the torus becomes optically thin (see also Sect. 4).

This can be illustrated with a simple order-of-magnitude estimate. The volume of the torus with half-opening angle  $\theta_{\text{trs}}$  within the radial limits  $r_{\text{in}}$  and  $r_{\text{out}}$  is  $V_{\text{trs}} = \frac{4\pi}{3}(r_{\text{out}}^3 - r_{\text{in}}^3) \cos \theta_{\text{trs}}$ . If we distribute the total mass contained in the stellar winds homogeneously in the volume of the torus, the number density of Hydrogene is

$$n_{\text{H}} = \frac{M_{\text{d,total}}}{1.4Z_{\text{d}}m_{\text{p}}V_{\text{trs}}}.$$

Integrating along the line of sight within the limits  $r_{\text{in}}$  and  $r_{\text{out}}$ , yields for the column density of such a homogeneous torus

$$N_{\text{H}} = \frac{3M_{\text{d,total}}}{5.6\pi Z_{\text{d}}m_{\text{p}}\cos\theta_{\text{trs}}}\frac{r_{\text{out}} - r_{\text{in}}}{r_{\text{out}}^3 - r_{\text{in}}^3} = 4.8 \times 10^{23} \text{ cm}^{-2}.$$

The total dust mass of the torus is  $350 M_{\odot}$  (see Eq. (18)) and for the geometry of the torus we used the same values as in Sect. 4, i.e.  $60^{\circ}$  for the half-opening angle and 1 and 5 pc for the inner and outer radius respectively. This gives less than half the column density of the patchy torus in Sect. 4, when the radiation pressure is strong enough to turn the wind back into elongated tails. Thus a torus with smoothly distributed matter would be optically thin, showing that a sufficiently high luminosity is necessary in order to maintain an optically thick torus. This is strengthened by our result from paper I, that for a merger of two BHs, each with  $10^8 M_{\odot}$  mass, more stars are required than for a merger of a  $10^8$  solar mass BH with one of 10 or even 100 times less mass. Thus more stars remain bound to the binary in a major merger and can build a more massive torus than in minor mergers. This is reasonable, since in a minor merger there will be a less massive stellar cluster surrounding the secondary BH, which is dragged to the common center by dynamical friction, than in a major merger.

Thus we come to the following conclusion: In a major merger with two BHs of comparable mass of about  $10^8 M_{\odot}$  more stars are brought during the merger of both galaxies to the common center and stay bound in the potential of the binary, where they enhance the optical thickness of the torus they constitute. Because of the stronger torque exerted by the BHs, the half-opening angle of this torus is larger than in a minor merger. Since the accretion rate is expected to be close to the Eddington limit, the stellar winds are exposed to strong radiation pressure from the center, which shapes the winds into elongated cometary tails, pointing radially away from the center. In this way they are sufficiently opaque as to make the stellar torus optically thick. With increasing time the accretion rate and therefore the luminosity will decrease, with the consequence that the stellar winds in the torus will become less collimated. Therefore the opacity of the torus will decrease also as an evolutionary effect of the AGN.

If, on the other hand, a  $10^8 M_{\odot}$  BH merges with a black hole of much less mass, less stars are involved and the torus will contain less stars. Because of the smaller torque of the binary, the torus is more diffuse and the opening angle is smaller. According to our simulation, such a torus looks like that of a major merger in early stages (compare the Figs. 2 and 14 in paper I). In such a minor merger also the accretion rate will be smaller and consequently the luminosity. This results in less radiation pressure acting on the stellar winds, which are not shaped into elongated tails, and thus the opacity of the torus, containing already fewer stars, is even more diminished.

This seems to be in agreement with the observations: Major mergers of galaxies of comparable size with BHs in their centers of comparable mass will violently stir up the stars, gas and dust, and finally assume an elliptical rather than a spiral shape. According to our finding above, ellipticals then should harbour AGN with tori having larger half-opening angles than spirals and thus on average Type 1 nuclei should be detected more often in

elliptical than spiral hosts. This is supported by the survey of Malkan, Gorjian, & Tam (1998), who find Seyfert 1 nuclei to reside on average in more early type hosts than Seyfert 2 nuclei.

It has been emphasized (i.e. Antonucci (2001a) and references therein) that there must be a range of covering factors for dusty tori, with the Type 2-classified objects having higher average covering factors. It is concluded that the populations are therefore intrinsically different in their statistical properties to some extent. Maybe the mass-ratio of the BHs and the evolution of AGN are the reasons for statistically different covering factors.

If the nucleus happens to be oriented to us in a way that the line of sight grazes the edge of the torus, the probability to see the nucleus still directly through a gap in the edge of the clumpy structure is more probable for large than small mass-ratios. This might be an explanation for NGC 4151, which is a Type 1 and has an aligned NLR too. But HST images show a cone on subarcsec scales (Antonucci 1993). According to the strict unified model this is not expected since a Type 1 should only be seen if the observer is inside the unobscured solid angle so that a projected ionization cone can not be seen. In our model the patchy torus can have gaps or holes, the more likely the larger  $q$  is and the closer the line of sight comes to the edge of the torus which is not clear defined. In the case of NGC 4151 the observer seems to be outside the opening angle. But through a gap in the torus close to its edge enough radiation can escape and is seen directly so that NGC 4151 is classified as a Type 1.

The nearest giant elliptical galaxy, M87 at redshift  $z = 0.0043$ , has been observed at  $10.8 \mu\text{m}$  wavelength by Perlman et al. (2001). If there is a dusty opaque torus it should be visible in the reradiated IR, but the authors find only little evidence of thermal emission from dust. Because of its large black hole mass ( $\sim 3 \times 10^9 M_{\odot}$ , Marconi et al. (1997)) and the giant elliptical shape it is likely to have undergone a major merger in the past. Since then the fuelling of the AGN probably has decreased and the luminosity dropped to its current estimated value of  $10^{42}$  erg/s (Whysong & Antonucci 2001), what fits to M87 being on the FR I-II border, as well in morphology as in radio power (Owen, Eilek, & Kassim 2000). This luminosity is then too weak as to maintain an opaque torus, which also might have been dissolved since the merger (see Sect. 4.2, lifetime of the torus). A possible minor merger afterwards most likely would not have sufficiently increased the luminosity and replenished the torus with stars in order to form a dusty and optically thick torus again. Whysong & Antonucci (2001) measured the reradiation from nuclear hot and warm dust, which must be emitted according to the unification scheme by the torus that absorbs the radiation from the AGN it surrounds. This radiation should be found in almost any hidden AGN and provides an estimate of the unblocked central luminosity. While for Cyg A at redshift 0.057 (more than 10 times the redshift of M87), with an estimated luminosity  $\sim 1.5 \times 10^{45}$  erg/s, they could detect this component, it is much weaker in M87, where

no hidden nucleus can be found. With respect to its large mass, M87 seems to host a starving black hole in the center.

This is in line with the results obtained by Meisenheimer et al. (2001), who compared galaxy-quasar pairs from the 3CR catalogue in the IR range from 5 to 180  $\mu\text{m}$  to test the unification scheme for luminous radio galaxies and quasars. The pairs have been selected such that they match in 178 MHz luminosity, which is thought to be emitted fairly isotropic, and redshift in order to minimize the effects of cosmic evolution. They can not distinguish the pairs by their mid- and far-infrared properties, what strongly supports the unification scheme. The authors also find the ratio of thermal dust power  $\nu F_\nu$ , averaged over 60 and 100  $\mu\text{m}$ , to the radio power at 178 MHz to correlate better with redshift than with luminosity. They suggest that this might be due to the thermal power of a radio source being primarily controlled by the accretion rate, which is supposed to be higher at large redshifts, when major mergers have been occurred more frequently than today.

## 9. Summary and conclusions

In paper I we showed that a central geometrically thick torus, comprised of stars, results at a distance of order 3 pc from the center as a product from the merger of two galaxies and their central supermassive black holes. This stellar torus has to be about as massive as the binary black hole in order to enable the BHs to get rid of their orbital angular momentum and to coalesce on scales of  $10^7$  yr.

In this present article we proved that this torus with its patchy structure is in very good agreement with the properties of the ubiquitous torus in AGN, as are demanded in the unification scheme and deduced from observations. About 1% of these stars have strong enough winds in order to obscure the central radiation source for lines of sight passing through their winds. The central radiation pressure shapes the winds of these obscuring stars in the torus into elongated tails, pointing radially away from the central source. Consequently their azimuthal extension is about  $4 \times 10^{-3}$  pc, such that these winds along their tails are optically thick, and that their total covering factor within the torus amounts to  $\sim 1$ . Thus these winds cause the geometrically thick torus also to be optically thick with column densities of about  $10^{24} \text{ cm}^{-2}$ , just as is observed. Also the inner radius of about 1 pc coincides with the evaporation radius of graphite dust grains (Lawrence 1991), what has been previously assumed to be the inner edge, and what is also the distance where the BHs become hard (Milosavljević & Merritt 2001) and which defined the inner edge in the simulation of paper I.

In Sect. 5 we demonstrated that the recent merging of two comparable supermassive BHs, the prerequisite for the forming of the opaque torus, can explain the X-shaped radio galaxies. According to the spin-paradigm, fast spinning BHs are powering strong radio jets in radio galaxies. If such a galaxy merges with another one hosting a

BH of comparable mass, the orbital angular momentum of the resulting BBH dominates over the maximum possible spin of the primary BH, at least till their major axis has shrunk to the last stable orbit. When the BHs eventually merge, the final spin might be dominated by the orbital angular momentum, leaving the merged BH spinning close to its maximum value. As a consequence a new powerful jet emanates into the direction of the orbital angular momentum, which is aligned with the symmetry axis of the torus. Therefore this jet streams through the ambient medium, producing strong radio emission, while the old jet's lobes, not fed anymore, are slowly fading away. The time scales of spectral aging of these lobes is close to the merger-time of the BHs and thus supports further this interpretation. The old jet might intersect with the torus and consequently would interact with its clumpy medium, also resulting in strong radio emission. This could be an explanation for the Compact Symmetric Objects, which are thought to be young and probably evolve into large-size Symmetric Objects, such as lower luminosity FR II double radio sources.

With such a patchy torus-model, the BAL QSOs fit well into the sequence in which a QSO appears as Blazar if seen pole. As the inclination angle increases it appears as normal quasar, then high ionization BAL QSO, low ionization BAL QSO and finally, when the line of sight lies in the equatorial plane of the torus, as ULIRG. For the intermediate angles the line of sight grazes the surface of the torus, explaining the features of the BAL QSOs. In the sample studied by Gallagher et al. (2002), for most of them a partial-covering absorber provides a significantly better fit than other models, confirming our torus model. The detected variability of the BAL quasar PG 2112+059 on scales of 6 yr is ascribed to changes in the absorber, probably the column density. This is just the time the stellar winds in the torus need to move through the line of sight. In Sect. 7 we give more examples of objects whose column densities are observed to change considerably on these time scales. They are very strongly supporting the idea of the patchy torus, since the winds of the stars, moving in the potential of the central BH, have the right size and optical depth in the appropriate distance to the center to yield such strong variations in  $N_{\text{H}}$  on the right time scales, as they move through the line of sight. Due to the stellar motion gaps in the torus will be continuously opened and closed.

For major mergers the resulting torus is more massive and therefore has a larger column density (see Sect. 8). Because the accretion-rate and consequently the luminosity will be higher than in minor mergers, the radiation pressure acting on the winds is stronger, being able to bend the winds into elongated tails. This further increases the torus' opacity compared to that of minor mergers. Since the torque of a more massive binary acting on the stars is stronger, the opening angle of the resulting torus is wider and therefore correlates with the central luminosity, as has been suggested in the past. But the column density of the torus will also change with time, as the luminos-

ity decreases when the accretion rate weakens. Thus the opacity depends on the mass-ratio of the merging black holes and on evolutionary effects of the AGN. Hence we expect to observe Type 1 AGN more likely in elliptical host galaxies at larger redshifts, where major mergers occurred more frequently. On the other hand this results on average in higher covering factors of Type 2 objects. In their survey of Seyfert galaxies Malkan, Gorjian, & Tam (1998) find on average Type 1 AGN to be hosted by more early type galaxies than Seyfert 2s, in agreement with our reasoning.

Previous compact torus models with a smooth distribution of the matter all faced the same problem in predicting a too narrow infrared spectrum, and to fit the data, additional NIR sources had to be invoked (Pier & Krolik 1993; Granato & Danese 1994; Efstathiou & Rowan-Robinson 1995; Alonso-Herrero et al. 2001). As is already mentioned in these papers, it is obvious that a patchy torus will tend to increase the dust temperature in the outer parts, since they are exposed to the radiation shining through gaps in the torus from the inner parts and the center. This will tend to broaden the IR spectrum. Such models also exhibit strong emission or absorption  $9.7\ \mu\text{m}$  Silicate features, which are usually not in agreement with the observations. Another problem is to achieve the geometrical thickness of the torus, which according to Pier & Krolik (1992b) can be supported by radiation pressure. But for a low luminosity source they need the torus to be clumpy and introduce a radiation pressure driven random motion of the clumps in order to maintain the thickness of the torus.

In the torus model we proposed here and in paper I, the torus is naturally thick as a result of the stars moving in the potential of the binary. The patchy structure inevitable leads to self-shielding of the stellar winds and also within the winds. This will probably have an effect on the temperature of the gas and dust as a function of the distance to the central source. Both, the selfshielding and the temperature distribution in the torus will have a strong influence on the reprocessed and reemitted radiation. The calculation of the temperature distribution and spectra of the winds and the torus they constitute would involve a full threedimensional treatment, so that radiation-transfer calculations are well beyond the scope of this paper and we can not give a comment on possible Silicate features as function of the inclination angle.

The torus model proposed in these two articles gives a coherent picture with respect to the formation of the torus, its evolution and application to observations in terms of the unification scheme.

*Acknowledgements.* CZ would like to thank R.R.J. Antonucci, M. Malkan, D. Merritt, G. Smith, and S. Westerhoff for their helpful discussions and their generous and kind hospitality. CZ also acknowledges the longterm support by the MPIfR. PLB would like to thank Drs. A. Donea and R. Protheroe for extended discussion on tori, and their hospitality at Adelaide. PLB also acknowledges the discussions with R.R.J. Antonucci, M. Malkan, G. Schäfer and N. Straumann. PLB and CZ also

like to especially thank M. Chirvasa for the discussions on her work of gravitational radiation of a black hole binary.

## References

- Alexander T., Netzer H., 1994, MNRAS, 270, 781  
 Alexander T., Netzer H., 1997, MNRAS, 284, 967  
 Alonso-Herrero A., Quillen A. C., Simpson C., Efstathiou A., Ward M. J., 2001, AJ, 121, 1369  
 Antonucci R., 1993, ARA&A, 31, 473  
 Antonucci R. R. J., 2001a, astro-ph/0110343  
 Antonucci R. R. J., 2001b, astro-ph/0103048  
 Antonucci R. R. J., Miller J. S., 1985, ApJ, 297, 621  
 Aretxaga I., Joguet B., Kunth D., Melnick J., Terlevich R. J., 1999, ApJ, 519, L123  
 Baribaud T., Alloin D., Glass I., Pelat D., 1992, A&A, 256, 375  
 Barthel P. D., 1989, ApJ, 336, 606  
 Barvainis R., 1987, ApJ, 320, 537  
 Biermann P., Harwit M., 1980, ApJ, 241, L105  
 Boller T., Fabian A. C., Sunyaev R., et al., 2002, MNRAS, 329, L1  
 Brotherton M. S., Tran H. D., van Breugel W., Dey A., Antonucci R., 1997, ApJ, 487, L113  
 Chini R., Kreysa E., Biermann P. L., 1989, A&A, 219, 87  
 Clavel J., Wamsteker W., Glass I. S., 1989, ApJ, 337, 236  
 Conway J. E., Blanco P. R., 1995, ApJ, 449, L131  
 Done C., Madejski G. M., Smith D. A., 1996, ApJ, 463, L63  
 Edwards A. C., 1980, MNRAS, 190, 757  
 Efstathiou A., Rowan-Robinson M., 1995, MNRAS, 273, 649  
 Egami E., Iwamuro F., Maihara T., Oya S., Cowie L. L., 1996, AJ, 112, 73  
 Engargiola G., Harper D. A., Elvis M., Willner S. P., 1988, ApJ, 332, L19  
 Fanti C., Fanti R., Dallacasa D., et al., 1995, A&A, 302, 317  
 Gallagher S. C., Brandt W. N., Chartas G., Garmire G. P., 2002, ApJ, 567, 37  
 Gallagher S. C., Brandt W. N., Laor A., et al., 2001, ApJ, 546, 795  
 George I. M., Mushotzky R., Turner T. J., et al., 1998, ApJ, 509, 146  
 Gilli R., Maiolino R., Marconi A., et al., 2000, A&A, 355, 485  
 Granato G. L., Danese L., 1994, MNRAS, 268, 235  
 Green P. J., Aldcroft T. L., Mathur S., Wilkes B. J., Elvis M., 2001, ApJ, 558, 109  
 Gregg M. D., Becker R. H., Brotherton M. S., et al., 2000, ApJ, 544, 142  
 Guainazzi M., Nicastro F., Fiore F., et al., 1998, MNRAS, 301, L1  
 Haas M., Müller S. A. H., Chini R., et al., 2000, A&A, 354, 453  
 Halpern J. P., 1982, Ph.D. Thesis, 4  
 Hoefner S., Fleischer A. J., Gauger A., et al., 1996, A&A, 314, 204  
 Huchra J., Burg R., 1992, ApJ, 393, 90  
 Hughes D. H., Robson E. I., Dunlop J. S., Gear W. K., 1993, MNRAS, 263, 607  
 Iwasawa K., Comastri A., 1998, MNRAS, 297, 1219  
 Iwasawa K., Fabian A. C., Matt G., 1997, MNRAS, 289, 443  
 Kartje J. F., 1995, ApJ, 452, 565  
 Kinney A. L., Antonucci R. R. J., Ward M. J., Wilson A. S., Whittle M., 1991, ApJ, 377, 100  
 Knapp G. R., Morris M., 1985, ApJ, 292, 640

- Krichbaum T. P., Alef W., Witzel A., et al., 1998, *A&A*, 329, 873
- Krolik J. H., Begelman M. C., 1988, *ApJ*, 329, 702
- Laurent O., Mirabel I. F., Charmandaris V., et al., 2000, *A&A*, 359, 887
- Lawrence A., 1991, *MNRAS*, 252, 586
- Longair M. S., 1981, *High energy astrophysics*. Cambridge: University Press, 1981
- Lovelace R. V. E., Romanova M. M., Biermann P. L., 1998, *A&A*, 338, 856
- Maccacaro T., Perola G. C., 1981, *ApJ*, 246, L11
- Macchetto F., Capetti A., Sparks W. B., Axon D. J., Boksenberg A., 1994, *ApJ*, 435, L15
- MacDonald J., Stanev T., Biermann P. L., 1991, *ApJ*, 378, 30
- Madejski G. M., 1998, in *Theory of Black Hole Accretion Disks*, p. 21
- Maiolino R., Salvati M., Bassani L., et al., 1998, *A&A*, 338, 781
- Malkan M. A., Gorjian V., Tam R., 1998, *ApJS*, 117, 25
- Marconi A., Axon D. J., Macchetto F. D., et al., 1997, *MNRAS*, 289, L21
- Mathis J. S., Rumpl W., Nordsieck K. H., 1977, *ApJ*, 217, 425
- Matt G., Fiore F., Perola G. C., et al., 1996, *MNRAS*, 281, L69
- Matt G., Guainazzi M., Frontera F., et al., 1997, *A&A*, 325, L13
- Meier D. L., 2001, *ApJ*, 548, L9
- Meisenheimer K., Haas M., Müller S. A. H., et al., 2001, *A&A*, 372, 719
- Merritt D., Ferrarese L., 2001a, *MNRAS*, 320, L30
- Merritt D., Ferrarese L., 2001b, *ApJ*, 547, 140
- Miller J. S., Goodrich R. W., Mathews W. G., 1991, *ApJ*, 378, 47
- Milosavljević M., Merritt D., 2001, *ApJ*, 563, 34
- Mulchaey J. S., Mushotzky R. F., Weaver K. A., 1992, *ApJ*, 390, L69
- Mushotzky R. F., 1982, *ApJ*, 256, 92
- Nagar N. M., Wilson A. S., 1999, *ApJ*, 516, 97
- Nandra K., Pounds K. A., 1994, *MNRAS*, 268, 405
- Niemeyer M., Biermann P. L., 1993, *A&A*, 279, 393
- Oliva E., Origlia L., Kotilainen J. K., Moorwood A. F. M., 1995, *A&A*, 301, 55
- Osterbrock D. E., Shaw R. A., 1988, *ApJ*, 327, 89
- Owen F. N., Eilek J. A., Kassim N. E., 2000, *ApJ*, 543, 611
- Owsianik I., Conway J. E., 1998, *A&A*, 337, 69
- Owsianik I., Conway J. E., Polatidis A. G., 1998, *A&A*, 336, L37
- Owsianik I., Conway J. E., Polatidis A. G., 1999, *New Astronomy Review*, 43, 669
- Pérez E., Márquez I., Marrero I., et al., 2000, *A&A*, 353, 893
- Parma P., Ekers R. D., Fanti R., 1985, *A&AS*, 59, 511
- Perlman E. S., Sparks W. B., Radomski J., et al., 2001, *ApJ*, 561, L51
- Peterson B. M., 1993, *PASP*, 105, 247
- Phillips R. B., Mutel R. L., 1982, *A&A*, 106, 21
- Pier E. A., Krolik J. H., 1992a, *ApJ*, 401, 99
- Pier E. A., Krolik J. H., 1992b, *ApJ*, 399, L23
- Pier E. A., Krolik J. H., 1993, *ApJ*, 418, 673
- Pogge R. W., 1989, *ApJ*, 345, 730
- Readhead A. C. S., Taylor G. B., Pearson T. J., Wilkinson P. N., 1996, *ApJ*, 460, 634
- Rees M., Silk J. I., Werner M. W., Wickramasinghe M. C., 1969, *Nat.*, 223, 788
- Reeves J. N., Turner M. J. L., Pounds K. A., et al., 2001, *A&A*, 365, L134
- Reichert G. A., Mushotzky R. F., Holt S. S., Petre R., 1985, *ApJ*, 296, 69
- Risaliti G., Maiolino R., Bassani L., 2000, *A&A*, 356, 33
- Rottmann H., Dennet-Thorpe J., Klein U., 1998, *Astronomische Gesellschaft Meeting Abstracts, Abstracts of Contributed Talks and Posters presented at the Annual Scientific Meeting of the Astronomische Gesellschaft at Heidelberg, September 14–19, 1998, poster #P77, 14, 77*
- Rowan-Robinson M., 1977, *ApJ*, 213, 635
- Rybicki G. B., Lightman A. P., 1979, *Radiative Processes in Astrophysics*. John Wiley & Sons
- Sanders D. B., Mirabel I. F., 1996, *ARA&A*, 34, 749
- Sanders D. B., Phinney E. S., Neugebauer G., Soifer B. T., Matthews K., 1989, *ApJ*, 347, 29
- Schmidt G. D., Hines D. C., 1999, *ApJ*, 512, 125
- Shull J. M., 1983, *ApJ*, 264, 446
- Singh K. P., Garmire G. P., Nousek J., 1985, *ApJ*, 297, 633
- Sitko M., 1991, in Miller H. R., Wiita P. J. (eds.), *Variability of Active Galactic Nuclei*. Cambridge University Press, p. 104
- Sprayberry D., Foltz C. B., 1992, *ApJ*, 390, 39
- Stecker F. W., Done C., Salamon M. H., Sommers P., 1991, *Physical Review Letters*, 66, 2697
- Taniguchi Y., Anabuki N., 1999, *ApJ*, 521, L103
- Tout C. A., Eggleton P. P., Fabian A. C., Pringle J. E., 1989, *MNRAS*, 238, 427
- Tsvetanov Z., Dopita M., Allen M., 1995, in *American Astronomical Society Meeting, Vol. 186, p. 4206*
- Turner M. J. L., Reeves J. N., Ponman T. J., et al., 2001, *A&A*, 365, L110
- Turner T. J., Perola G. C., Fiore F., et al., 2000, *ApJ*, 531, 245
- Turner T. J., Pounds K. A., 1989, *MNRAS*, 240, 833
- Turner T. J., Weaver K. A., Mushotzky R. F., Holt S. S., Madejski G. M., 1991, *ApJ*, 381, 85
- Ueno S., Koyama K., Nishida M., Yamauchi S., Ward M. J., 1994, *ApJ*, 431, L1
- Urry C. M., Padovani P., 1995, *PASP*, 107, 803
- Uttley P., McHardy I. M., Papadakis I. E., Cagnoni I., Fruscione A., 1998, in *The Active X-ray Sky: Results from BeppoSAX and RXTE. Proceedings of the Active X-ray Sky symposium, October 21-24, 1997, Rome, Italy*, Edited by L. Scarsi, H. Bradt, P. Giommi, and F. Fiore. Publisher: Amsterdam: Elsevier, 1998. Reprinted from: *Nuclear Physics B, (Proc. Suppl.)*, vol. 69/1-3. ISBN: 0444829903., p.490, p. 490
- Voit G. M., Shull J. M., 1988, *ApJ*, 331, 197
- Voit G. M., Weymann R. J., Korista K. T., 1993, *ApJ*, 413, 95
- Warwick R. S., Sembay S., Yaqoob T., et al., 1993, *MNRAS*, 265, 412
- Weaver K. A., Nousek J., Yaqoob T., et al., 1996, *ApJ*, 458, 160
- Weymann R., 1997, in *ASP Conf. Ser. 128: Mass Ejection from Active Galactic Nuclei*, p. 3
- Weymann R. J., Morris S. L., Foltz C. B., Hewett P. C., 1991, *ApJ*, 373, 23
- Whyson D., Antonucci R. R. J., 2001, *astro-ph/0106381*
- Wilkinson P. N., Polatidis A. G., Readhead A. C. S., Xu W., Pearson T. J., 1994, *ApJ*, 432, L87
- Willott C. J., Rawlings S., Blundell K. M., 1999, in *ASP Conf. Ser. 162: Quasars and Cosmology*, p. 135
- Wills B. J., 1999, in *ASP Conf. Ser. 162: Quasars and Cosmology*, p. 101

- Wilson A. S., Braatz J. A., Heckman T. M., Krolik J. H., Miley G. K., 1993, ApJ, 419, L61
- Wilson A. S., Colbert E. J. M., 1995, ApJ, 438, 62
- Wilson A. S., Tsvetanov Z. I., 1994, AJ, 107, 1227
- Winters J. M., Dominik C., Sedlmayr E., 1994, A&A, 288, 255
- Xue S., Otani C., Mihara T., Cappi M., Matsuoka M., 1998, PASJ, 50, 519
- Young P. J., Shields G. A., Wheeler J. C., 1977, ApJ, 212, 367
- Zier C., Biermann P. L., 2001, A&A, 377, 23, (paper I)